Implementation of Intelligent Controller for Three Phase Vector Controlled Induction Motor

A Dissertation Submitted In Partial Fulfillment of the Requirements for the Award of Degree of

MASTER OF TECHNOLOGY

IN

CONTROL AND INSTRUMENTATION

Submitted by

SHOEB HUSSAIN

2K11/C&I/13

Under the Esteemed Guidance of

PROF. MADHUSUDAN SINGH

ELECTRICAL ENGINEERING DEPARTMENT

DELHI TECHNOLOGICAL UNIVERSITY

(FORMERLY DELHI COLLEGE OF ENGINEERING)

BAWANA ROAD, DELHI-110042

JULY – 2013

DELHI TECHNOLOGICAL UNIVERSITY

DEPARTMENT OF ELECTRICAL ENGINEERING

Certificate

This is to certify that the thesis entitled, "**Implementation of Intelligent Controller for Three phase Vector Controlled Induction Motor**", has been done in partial fulfillment of the requirements for award of the degree in M.Tech in Control & Instrumentation under my supervision by Shoeb Hussain (2K11/C&I/13), at the Delhi Technological University.

This work has not been submitted earlier in any university or institute for the award of any degree to the best of my knowledge.

(Prof. Madhusudan Singh)
Department of Electrical Engineering

Acknowledgement

All thanks to Almighty Allah for this piece of work.

I am greatly thankful to the Electrical Engineering department of Delhi Technological University for giving me an opportunity to present myself and perform in this institution.

I would like to thank Prof. Madhusudan Singh, the Head of the Department, Electrical Engineering and also my project guide, who suggested & constantly encouraged me to complete the project in time.

I am also thankful to Dr. A.H. Bhat, my B.Tech teacher, who has provided me with a great knowledge in the field of power electronics. I am also thankful to all my teachers who provided me with the knowledge of control systems and electrical machines throughout my study at the Delhi Technological University.

I would like to thank Mr. Ajender Singh (Junior Machine Lab) and Mr. Karan Singh (Control System Lab), technical staff, who helped me in arranging the equipments necessary to complete my project work.

I also am thankful to my classmates, my friends for being right behind me throughout my M.Tech course at the Delhi Technological University.

The work has been taken from many references and sources of information.

Here I would whole heartedly like to thank all above for helping me.

And not at all the least, I am thankful to my family, especially my parents for all that they have done for me throughout my life and also during my course at the Delhi Technological University, far away from me, always remembering me in their prayers.

Shoeb Hussain

Roll no. 2K11/C&I/13

M.Tech (Control & Instrumentation)

Abstract

Induction motors are widely used in industry due to the fact that they are relatively cheap, rugged and require less maintenance. In the past few decades various control methods have been reported to control torque and speed of three phase Induction motor. The Vector control has widespread use in high performance induction motor drives. It allows a decoupled control of electromagnetic torque control and the motor flux, and hence the induction motor is operated as DC motor. In this technique, the variables are transformed into a reference frame in which the dynamic variables behave like DC quantities. The decoupling control between the flux and torque allows induction motor to achieve fast transient response. Therefore, it is preferred used to use it in high performance motor applications.

The motivation behind this project is to implement an intelligent control scheme for a three phase vector controlled induction motor drive. The speed controller is employed in the outer loop. The complete vector control scheme of the IM drive incorporating a PI-Controller & an FLC is experimentally implemented using a digital signal processor board DS-1104 in the laboratory on a 3-hp, 230 V, 1440rpm, 3 phase Induction motor. A comparison of the drive performance using a conventional PI and an intelligent Fuzzy Logic controller is presented through simulation in MATLAB/SIMULINK as well as through real time implementation of the scheme.

List of Symbols used

d^e-q^e	Synchronously rotating reference frame direct and quadrature axes
d^s-q^s	Stationary reference frame direct and quadrature axes
f	Frequency (Hz)
I_f	Machine field current.
I_s	Rms stator current.
I_d	DC Current
i_{dr}^s	d^s axis rotor current
i_{ds}^s	d^s axis stator current
i_{qr}	q^e - axis rotor current
i_{qs}	q^e - axis stator current
L_m	Magnetizing inductance
L_r	Rotor inductance
L_s	Stator inductance
L_{lr}	Rotor leakage inductance
L_{ls}	Stator leakage inductance
L_{dm}	d^e- axis magnetizing inductance
L_{qm}	q^e axis magnetizing inductance
N_e	Synchronous speed (rpm)
N_r	Rotor speed(rpm)
P	Total number of poles
s	Slip

T_e	Developed torque
V_d	DC voltage
$\Psi_{dr}{}^{s}$	d^s- axis rotor flux linkage
$\Psi_{ds}{}^{s}$	d^s- axis stator flux linkage
Ψ_{qr}	q^e - axis rotor flux linkage
Ψ_{qs}	q^e- axis stator flux linkage
ω_e	Stator or line frequency (r/s) Rotor mechanical speed
ω_r	Rotor electrical speed
ω_{sl}	Slip frequency
Θ_{sl}	Slip angle
Θ_r	Rotor angle
R_s	Stator Resistance/phase
R_r	Rotor Resistance/phase

List of Figures

Table of Contents

Chapter I

Introduction

1.1 General

Drives today have become an important part of the modern industry. The motor drives are used in very wide power range. They are used in applications where power requirement varies from few watts to many thousands of kilowatts. Besides these, applications range from very precise, high-performance position-controlled drives in robotics to variable-speed drives for adjusting flow rates in pumps, blowers and fans. In all these applications where speed and position control is of great significance, the drives are controlled via a power electronic converter, an interface between the input power and the motor.

Induction motors are most widely used in drive systems. Induction motors with squirrel-cage rotors are the workhorse of modern industry owing to their low cost, rugged construction and less maintenance. Induction motor is a complex higher-order, nonlinear, strongly coupled, and multi-variable system. When operated directly from the line voltages, an induction motor operates at a nearly constant speed. However, by means of power electronic converters, it is possible to vary the speed of an induction motor.

As a consequence of the wide range applications of the induction motor, much attention has been given to motor torque and speed control. Its main speed-controller patterns could be classified as: slip power consumer, slip power feeder and fixed slip power. On an application where dynamic control is not in issue, the control requirement of the AC machine drive has been done using constant *'voltshertz (V/f)'* technique. However, with the advancements in induction motor modelling, high performance and lower loss switching, power electronic devices and microprocessors, the development of high performance AC drives has become a reality**.**

The two main types of high performance AC drives are, field oriented and direct torque control (DTC) drives. These drives have various applications that previously have been

dominated and reserved for DC motors and drive systems. Vector control belongs to the fixed slip power pattern. It is the typical representative method for high efficiency. The stator current of induction motor could be decomposed to field current component and torque current component with dynamic mathematical model and coordinate transformation. The two components could be controlled independently to achieve good dynamic response, which is similar to the control pattern of the DC motor.

Besides the advent of power electronic converters, the improvement in control techniques have resulted in better dynamic response of the motor characteristics. The P, PI, PID speed controllers are now being replaced with Intelligent Control techniques like Fuzzy, Neural Network etc. The use of these intelligent controllers has resulted in improvement in the drive system performance.

In this work, a fuzzy logic speed controller has been applied on a vector controlled induction motor drive. The performance of the drive with and without intelligent controller has been analysed in real time & compared with the performance obtained through simulation in MATLAB/Simulink.

1.2 Literature Survey

At the present time, the field oriented control (FOC) technique or Vector control has widespread use in high performance induction motor drives. It allows, by means of co-ordinate transformation, to decouple the electromagnetic torque control from the rotor flux, and hence induction motor acts as a DC motor. In this technique, the variables are transformed into a reference frame in which the dynamic variables are like DC quantities. The decoupling control between the flux and torque allows induction motor to achieve fast transient response. Therefore, it is preferably used in high performance motor applications. Field Oriented control uses a vector model of the drive which is valid during transient operation also, which facilitates faster control of the drive. An extensive literature review of various emerging intelligent control techniques and methods of speed/torque control of three phase Induction motor has been presented.

1.2.1 Indirect Vector Control

There are essentially two general methods of vector control. One, called the direct or feed- back method, was invented by Blaschke [1], and the other, known as the indirect or feedforward method was invented by Hasse [2, 4].The two methods differ in the way the rotor angle is determined. In direct FOC the angle is obtained by the terminal voltages and currents, while as in indirect FOC, the angle is obtained by using rotor position measurement and machine parameter's estimation.

Field orientation has emerged as a powerful tool for controlling ac machines such as inverter-supplied induction motors/synchronous motors. The dynamic performance of such drives is comparable to that of a converter fed four quadrant dc drives. The complex functions required by field oriented control are executed by intelligent controllers using microcontrollers or digital signal processors (DSP), thus greatly reducing the necessary control hardware [3, 6].

An important requirement to obtain good control performance is to make the motor parameters in the field-oriented controller coincide with the actual parameters of the motor. The ability to inject currents into the motor with a current source opened up new possibilities for parameter determination. It was Takayoshi [4] who described a new identification technique utilizing injected negative sequence components. It is shown that the stator as well as rotor resistance and leakage inductance can be determined on line while the motor is driving the load. The theory is verified with a full-scale hybrid computer simulation of a field-oriented controlled PWM inverter based induction motor drive.

The performance of induction motor drive is mainly determined by the gating pulses feeding the inverter and hence the output current generated by the inverter. A current control technique using hysteresis [5, 9] can be applied for determining the pulse pattern. With this method, fast response current loop is obtained and knowledge of load parameter is not required. However this method can cause variable switching frequency of inverter and produce undesirable harmonic generation. A new Space vector current control technique, proposed by Ting–Yu et.al.[16], for induction motor drive, shows better

performance. No time-varying coordinate transformation and no complicated calculation are required. It is described that even a simple 8751 microcomputer is used to implement a high-performance drive system. In addition, the proposed space vector-based current controller uses the extra information of error derivative to reduce the switching frequency greatly.

For Speed controllers, mostly conventional PI control technique has been used. But with advancement in control strategies, a number of controllers have been proposed over the years. The use of H_2 and $H\infty$ control technique implementation in vector control scheme, proposed by Yau-Tze et.al [13], have shown better disturbance rejection capability than a PI controller and, in particular, $H\infty$ controller performs the best.

The fixed gain controllers are very sensitive to parameter variations, load disturbances etc. Other techniques may involve the use of soft computing techniques like fuzzy logic controllers. There are some advantages of fuzzy logic controller as compared to conventional PI, PID and adaptive controller such as it does not require any mathematical model, it is based on linguistic rules within IF-THEN general structure, which is the basic of the human logic. Fuzzy Logic Controller has found its application in vector controlled induction motor drive replacing PI controllers. Gilberto et.al [20] proposed a fuzzy logic based on-line efficiency optimization control for an indirect vector controlled drive system. The method uses a fuzzy controller to adjust adaptively the magnetizing current based on the drive measured input power, thus yielding true optimum efficiency operation with fast convergence. Fast convergence is achieved by using adaptive step size of the excitation current. The low-frequency pulsating torque generated by the efficiency controller has been suppressed by a feedforward compensation algorithm.

Emanuele [29] proposed a fuzzy adaptive control scheme for vector controlled induction motor drive. The neuro-fuzzy approach is presented and used to develop a semiautomatic procedure to optimize such adaptive fuzzy laws. The design of the adaptive fuzzy laws is presented on the basis of some linguistic rules that describe the expected behavior of the adapting process. Results from the same showed superior performance over conventional techniques.

D-space implementation of the vector control scheme for induction motor drive resulted in confirmation of the results in real time for rapid control prototyping (RCP). The real-time hardware, based on a PowerPC microprocessor and its I/O interfaces make the board ideally suited for developing controllers in various fields, in both industry and university. A new Fuzzy Logic Controller design was presented by M.Nasir-uddin [40].The fuzzy-logic speed controller is employed in the outer loop. The complete vector control scheme of the IM drive incorporating the FLC is experimentally implemented using a digital signal processor board DS-1102 for the laboratory 1-hp squirrel-cage IM. In order to minimize the real-time computational burden, simple membership functions and rules have been used. It is concluded that the proposed FLC has shown superior performances over the PI controller.

In the present work, the above limitation of real time burdening has been removed and a detailed membership function input scheme for FLC is implemented to improve the system performance.

The Space Vector Pulse Width Modulation (SVPWM) method is an advanced, computation-intensive PWM method and possibly the best among all the PWM techniques for variable frequency drive application. This technique have better dc bus utilization and easy for digital implementation. A space-vector-based current-regulated PWM inverter with new switching tables was designed and implemented by Yi-Hwa Liu et.al [30]. Due to full utilization of all available voltage vectors, current harmonic contents have been improved by the proposed switching table in the angular coordinate.

New Optimisation techniques are proposed in [42, 45]. Such hybrid techniques ensure high performance drives.

1.2.2 Direct Vector Control

It was Blaschke [1], who first proposed direct vector control. In direct FOC the rotor angle or control vector is obtained by the terminal voltages & currents directly by using flux estimators. The direct vector control is also known as feedback vector control scheme.

Similar to Indirect Vector Control, various controllers have been implemented on direct vector controlled induction motor drives also to improve the performance of the drive.

While the direct method is inherently the most desirable control scheme, it suffers from high cost and the unreliability of the flux measurement. Although the indirect method can approach the performance of the direct measurement scheme, the major weakness of this approach is centered upon the accuracy of the control gains which, in turn, depend heavily on the motor parameters assumed in the feedforward control algorithm [4].

Neural networks are recently showing good promise for application in power electronics and motion control systems. M. Godoy et.al [21] proposed a feedforward neural network technique for estimation of feedback signals of a direct vector-controlled (DVC) induction motor drive. The neural network estimator showed the advantages of faster execution speed, harmonic ripple immunity, and fault tolerance characteristics compared to DSP-based estimator.

Susumu [25] et.al proposed a combined feedforward and feedback (FF/FB) control to improve robustness of vector controlled induction motors. This FF/FB system maintains the quick response of the slip-frequency-type and is insensitive to parameter variation in cooperation with field-orientation control. Furthermore a Neural network Controller is proposed for controlling the dynamics of the drive. The neuro-based technologies contribute to provide an adjustment-free and maintenance-free vector-controlled induction motor for the industrial fields.

Bimal.K.Bose et.al [26] extended the fuzzy efficiency optimization control to a stator flux-oriented direct vector-controlled electric vehicle (EV) induction motor drive of 100-kW power. The fuzzy controller input– output transfer characteristics are then used to train a feedforward neural network with delayed feedback, which then replaces the fuzzy controller in the drive system. Such a neuro–fuzzy control combines the advantages of fuzzy and neural controls. The control attains fast convergence with inherent adaptive step size signals of fuzzy control. The neural network implementation permits fast computation and can be implemented by a dedicated hardware chip or by DSP-based software. Extensive simulation study verifies excellent performance of the controller.

1.2.3 Direct Torque Control

This involves calculating an estimate of the motor's magnetic flux and torque based on the measured voltage and current of the motor. Ultimately the aim is to control the speed of the motor.

Isao Takahashi and Toshihiko Noguchi described a control technique termed DTC in an IEEJ paper presented in September 1984 and in an IEEE paper published in late 1986 [7]. The proposed scheme is based on limit cycle control of both flux and torque using optimum PWM output voltage; a switching table is employed for selecting the optimum inverter output voltage vectors so as to attain as fast a torque response, a low inverter switching frequency, and low harmonic losses as possible. The efficiency optimization in the steady-state operation is also considered; it can be achieved by controlling the amplitude of the flux in accordance with the torque command.

Again Isao Takahashi in 1989 [8] proposed a better performance DTC control scheme. This paper proposes new control schemes based on the principle of Arago's disk, which can be considered a basic law of torque generation in the induction motor. It makes possible both fast torque response and high-efficiency control at the same time. In the system, instantaneous values of the flux and the torque are calculated from primary variables and controlled independently by using an optimum switching table. Therefore, it can achieve not only the fastest torque response but also the lowest harmonic losses and acoustic noise.

Marian in 1995 [22] showed how by introducing an additional carrier signal to the torque controller input, the robust start and improved operation at low speed region can be achieved. There is no separate voltage modulation block. There are no current regulation loops. Coordinate transformation is not required. There is no need for a voltage decoupling network.

A torque control scheme, based on a direct torque control (DTC) algorithm using a 12-sided polygonal voltage space vector, was proposed for a variable speed control of an open-end induction motor drive, by Chintan et.al [64]. The proposed DTC scheme selects

switching vectors based on the sector information of the estimated fundamental stator voltage vector and its relative position with respect to the stator flux vector. The proposed DTC scheme utilizes the exact positions of the fundamental stator voltage vector and stator flux vector to select the optimal switching vector for fast control of torque with small variation of stator flux within the hysteresis band. The present DTC scheme allows full load torque control with fast transient response to very low speeds of operation, with reduced switching frequency variation.

1.2.4 Sensorless Vector Control

Sensorless Vector Control schemes do not implement any speed sensor. A Speed encoder is undesirable because it increases cost & reliability problems. Estimation of speed is possible from machine terminal voltages & currents. Even though, the sensorless vector control method adds to complexity, but reliability can be achieved through various estimation algorithms available.

Tsugutoshi [12] proposed a vector-control scheme based on a rotor-flux speed control, which involves torque-producing current and rotor flux, derived from the stator voltages and currents. In the proposed rotor-flux estimator, a lag circuit is employed, to which both the motor-induced voltage and the rotor-flux command are imposed, and therefore it is possible to calculate even a low frequency down to standstill. Selecting the rotor-flux estimator parameter to set the same time constant to the lag circuit as that of the rotor-circuit is considered to reduce the influence of stator resistance. The proposed system can be controlled precisely over a wide speed and load range.

Colin [14] proposed a development of Model Reference Adaptive System (MRAS) for the estimation of induction motor speed from measured terminal voltages & currents. The new MRAS scheme is thought to be less complex and more effective.

Fang-Zheng [19] described a new approach to estimating induction motor speed from measured terminal voltages and currents for speed-sensorless vector control. The proposed approach is based on observing the instantaneous reactive power of the motor. The estimated speed is used as feedback in an indirect vector control system. The new

approach is not dependent upon the knowledge of the value of the stator resistance, nor is it affected by stator resistance thermal variations. Furthermore, pure integration of sensed variables, in principle, is not required at all. Therefore, this new method can achieve much wider bandwidth speed control than previous tacholess drives.

Joachim [39] et.al proposed a new approach for speed estimation through stator flux integration. A pure integrator is employed for stator flux estimation which permits high-estimation bandwidth. Compensation of the drift components is done by offset identification. The nonlinear voltage distortions are corrected by a self-adjusting inverter model. A further improvement is a novel method for online adaptation of the stator resistance. Experiments demonstrated smooth steady-state operation and high dynamic performance at extremely low speed.

Epaminondas et.al [37] proposed a new simple algorithm capable of running in a low-cost microcontroller, which is derived from the dynamic model of the induction machine. Assuming that flux calculation errors are due to stator resistance variations, the estimation algorithm corrects the stator resistance value in order to eliminate the error. It has been proven that, with the proposed method, an accurate estimation of the stator flux is achieved. As a result of this, torque control can be precise, even in the low-speed range, offering good dynamic performance of the asynchronous machine.

1.3 Objectives of the Present Work

The main objective of the present work is to implement an intelligent control scheme for a three phase vector controlled induction motor. The speed control of the motor is achieved under different operating conditions and compared by implementing two control schemes,

i) PI controller
ii) Fuzzy Logic Controller

The complete indirect vector control strategy has been implemented in hardware by the use of DS-1104. The performance of the hardware results is validated with the results obtained through simulation in MATLAB/Simulink.

1.4 Conclusion

The vector control scheme for induction motor control had tremendous progress over the years. With the advent of Control techniques like Fuzzy and Neural network, it has been possible to control the speed of motor in a more efficient and effective manner. The use of microprocessors for controlling the speed or the use of Digital Signal Process Kits has made it possible to control the motor dynamics in real time.

The outline of the dissertation consists of the dynamic modeling of induction motor and the vector control scheme, described in Chapter 2. In Chapter 3, the PI & FLC controllers are studied along with the hardware components. The results from the work implemented through simulation in MATLAB as well as through hardware implementation are presented in Chapter 4. Chapter 5 presents main conclusion and future scope of the work.

Chapter II

Dynamics of Vector controlled Induction Motor

2.1 Introduction

A three phase induction motor is shown in Fig. 2.1. It consists of a stator with stator windings and a rotor. The stator carries a 3-phase stator winding. The rotor of the three phase induction motor is either wound type, consists of three phase winding or squirrel-cage type consisting of shorted end rings. There is a small air gap between the stator and the rotor, the size of which depends upon the power rating of the motor. Induction motor is known as asynchronous motor because the induction motor operation comes from the slip between the rotational speed of the stator field and somewhat slower speed of the rotor.

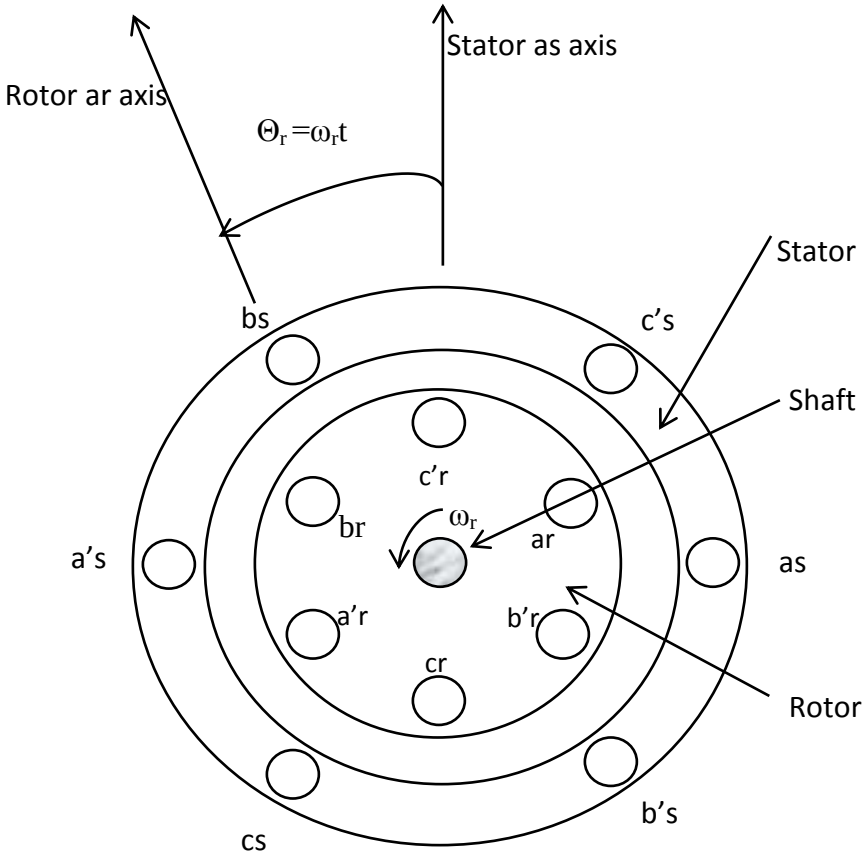

Fig. 2.1 Representation of a three phase induction motor

The principle of operation of any induction motor is the production of magnetic field by the motor windings due to sinusoidally distributed flux over the circumference of the rotor. Depending on the supply frequency and the number of poles on the winding the field rotates in space about the circumference of the machine at a rate termed the 'synchronous speed'. The rotating field is produced by properly arranging a stator winding such that each phase occupies 360/n electrical degrees of the stator circumference, where n is the number of phases of the exciting voltage.

A sinusoidal three-phase balanced power supply in the three-phase stator winding creates a synchronously rotating magnetic field. Each phase winding will independently produce a sinusoidally distributed mmf (magneto- motive force) wave, which pulsates about the respective axes. Consider the superposition of three coplanar magnetic field intensities, at a point in space where the three field intensities are displaced 120^o in space and 120^o in time. Each of the three components of magnetic field is uniform with respect to the space coordinates.

When the rotor is subjected to magnetic field, emf is induced in the rotor. This induced current results in the production of torque in the motor. At synchronous speed of the machine, the rotor cannot have any induction and therefore torque cannot be produced. At any other speed N_r, the speed differential N_s- N_r called slip speed, induces rotor current and torque is developed. The rotor moves in the same direction as that of the rotating magnetic field to reduce the induced current. Basic to the operation of induction motor control is the control of speed or torque by controlling the slip and control of flux by controlling voltage or current.

In this chapter, the different control techniques of induction motor drives, including scalar control, vector control have been described.

2.2 Induction Motor Control

Squirrel cage induction machines are simple and rugged and are considered to be the workhorses of industry. At present induction motor drives dominate the world market. However, the control structure of an induction motor is complicated since the stator field

is revolving, and further complications arises due to the fact that the rotor currents or rotor flux of a squirrel cage induction motor cannot be directly monitored.

The control and estimation of ac drives in general are considerably more complex than those of dc drives, and this complexity increases substantially if high performances are demanded [67]. The main reasons for this complexity are the need of variable-frequency, harmonically optimum converter power supplies, the complex dynamics of ac machines, machine parameter variations, and the difficulties of processing feedback signals in the presence of harmonics. However by using fundamental physical laws or space vector theory, it is easy to show that, similar to the expression of the electromagnetic torque of a separately exited dc machine, the instantaneous electromagnetic torque of an induction motor can be expressed as the product of a flux producing current and a torque producing current, if a special flux oriented reference is used.

The Induction motor Control techniques have been broadly grouped into two main categories. These are

I. Scalar Control
II. Vector Control

2.2.1 Scalar Control

Scalar control is a relatively easier control method. It involves the change in the magnitude variation of the control parameters. The control method involves the control of flux and torque. By controlling the voltage of the machine, it is possible to control the flux of the motor. Also by controlling the frequency of the motor, it is possible to control the torque. However, the decoupling effect is not taken into consideration. The change in control parameters of either voltage or frequency also leads to change in torque and flux respectively, as torque and flux are also dependent on voltage and frequency. Scalar control is in contrast to vector or field-oriented control (will be discussed later) where both the magnitude and phase alignment of vector variables are controlled. Scalar-controlled drives give somewhat inferior performance but they are easy to implement. However their importance has diminished recently because of the

superior performance of vector-controlled drives which is demanded in many applications.

Many types of Scalar Control techniques are available in literature. The speed and torque can be varied using one of the following means:

I. Stator Voltage Control
II. Rotor Voltage Control
III. Frequency Control
IV. Stator Voltage and Frequency Control
V. Stator Current Control
VI. Voltage, Current & Frequency Control

Out of these all, Stator Voltage and Frequency Control is the most acceptable one and widely used. The stator voltage and frequency control is to control the induction motor speed and torque by varying the ratio of voltage to frequency that use to supply to the stator. If the ratio of voltage to frequency is kept constant, the flux will remain constant. This will prevent the saturation of air gap flux due to the increases in flux. By keeping the ratio of voltage to frequency constant, this technique allows the induction motor to deliver its rated torque at speeds up to its rated speed. This control system needs voltage boost when operated at low frequency. This is because; the air gap flux is reduced due to the drop in the stator impedance when motor operates at a low frequency.

2.2.2 Vector Control

Scalar control techniques have been well known and easier to implement, but the inherent coupling effect (i.e. both torque and flux are functions of voltage or current and frequency) gives the sluggish response and the system is easily prone to instability because of high order system harmonics [67]. For example, if the torque is increased by incrementing the slip, the flux tends to decrease. The flux variation is sluggish. The flux variation is then compensated by the sluggish flux control loop feeding in additional voltage. This temporary dipping of flux reduces the torque sensitivity with slip and lengthens the system response time.

The problems involved with scalar control were eliminated by the invention of Vector control. In 1970's, Blaschke [1] and Hasse [2], developed the concept of Vector control or Field Oriented control (FOC), in two different fashions, the Direct FOC and the Indirect FOC. The concept behind the vector control is to control the induction motor similar to that of a separately excited DC motor. Because of DC machine like performance, vector control is known as decoupling, orthogonal or transvector control [67]. The processing of vector control, however, is very complex and requires the use of high speed microcontrollers and Digital Signal processors (DSP).

The theory of vector control is discussed later in this chapter.

2.3 Dynamics of Induction Motor Control

The steady state model of induction motor, which is represented by an equivalent circuit of induction motor, describes the only steady state behaviour of the induction motor. It is used when steady state analyses of Induction motor, such as efficiency, losses, steady state torque, currents and fluxes are to be evaluated. Designing the machine drives based on the steady state model will only result in the production of a drive that normally has a poor transient performance. When machine drives for high performance applications need to be designed, a model that can describe the transients as well as the steady state behaviour of the induction machine is needed. Therefore, by using the dynamic model, the transient behaviour of the induction motor, which cannot be analysed using steady state equivalent model, can be predicted and studied. The dynamic model of induction motor involves the transformation of axes from abc to dq. This transformation of axes is the basis of Induction motor vector control strategy.

The dynamic model of a three phase squirrel cage induction motor in synchronously rotating reference frame is shown in Fig 2.2. The model shows the quadrature and direct axis components of current flowing through the stator windings and the rotor of the Induction motor.

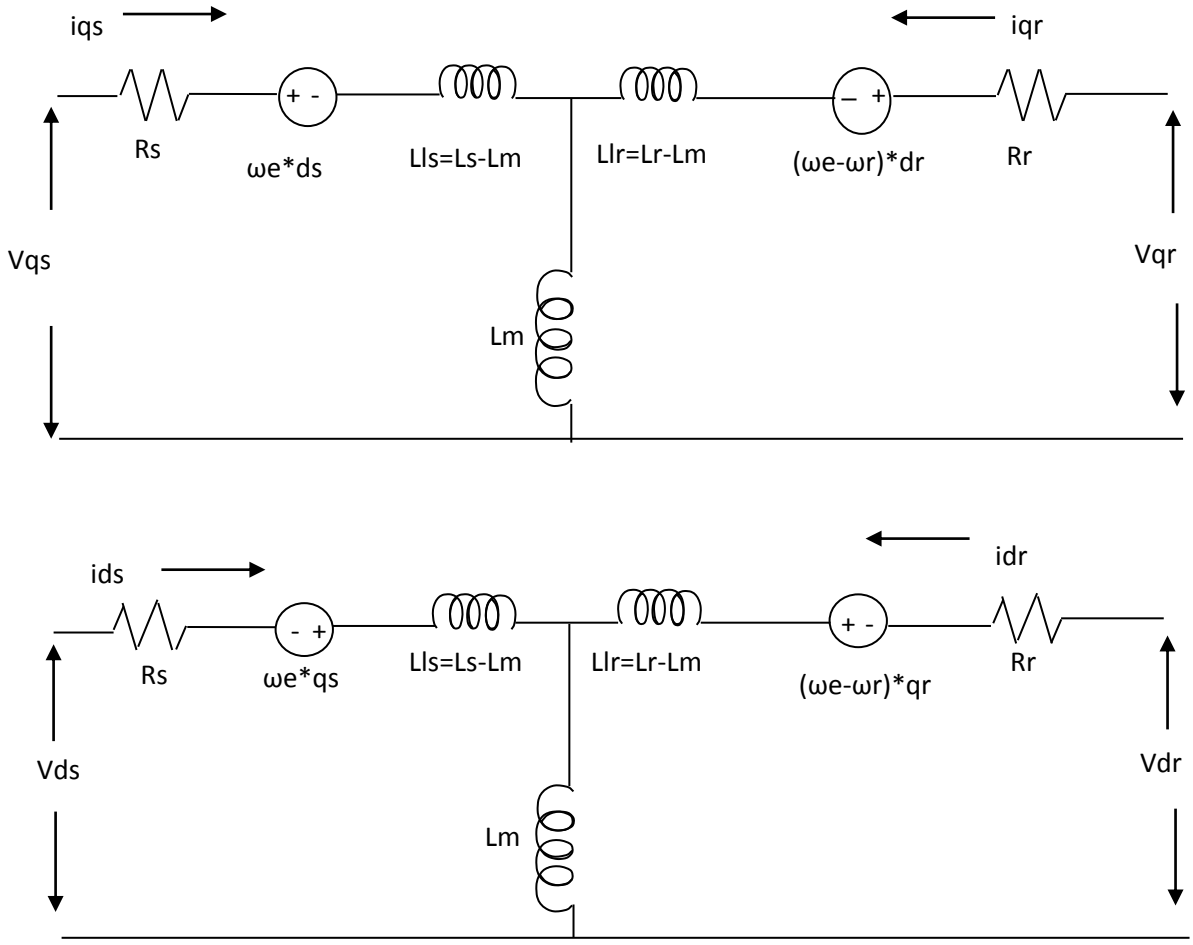

Fig. 2.2 Equivalent circuit of Induction motor in a synchronously rotating reference frame, a) quadrature-axis circuit b) direct-axis circuit

The dynamic model of the induction motor is obtained by axes transformation proposed by Park in 1920's. Park formulated a change in variables. By the change of these variables, the voltage, current and flux variables, associated with stator winding, are replaced with fictitious variables of a winding rotating with the rotor at synchronous speed. Park transformed, or referred, the stator variables to a '*synchronously rotating reference frame'* fixed in the rotor. With such a transformation (called Park's transformation), he showed that all the time-varying inductances that occur due to an electric circuit in relative motion and electric circuits with varying magnetic reluctances can be eliminated [67]. Later, in the 1930s, H. C. Stanley [67] showed that time-varying inductances in the voltage equations of an induction machine due to electric circuits in relative motion can be eliminated by transforming the rotor variables to variables

associated with fictitious stationary windings. In this case, the rotor variables are transformed to a '*stationary reference frame'* fixed on the stator. Later, G. Kron [67] proposed a transformation of both stator and rotor variables to a synchronously rotating reference frame that moves with the rotating magnetic field. D. S. Brereton [67] proposed a transformation of stator variables to a '*rotating reference frame'* that is fixed on the rotor. In fact, it was shown later by Krause and Thomas [67] that time-varying inductances can he eliminated by referring the stator and rotor variables to a common reference frame which may rotate at any speed '*arbitrary reference frame*'.

2.3.1 Axes Transformation

The *abc-dq* transformation is an essential part of this scheme. The direct–quadrature–zero (or *dq*0) transformation or zero–direct–quadrature (or 0*dq*) transformation is a mathematical transformation used to simplify the analysis of three-phase circuits.

The transformation of abc - dq involves the decoupling of variables with time-varying coefficients and refer all variables to a common reference frame. This transformation reduces the three line currents to two DC quantities in dq reference frame. The two DC quantities are orthogonal to each other. This allows the control of the two quantities independently.

The three-phase transformation into two-phase is carried out through *abc-dq* transformation by using various methods like Stanley's transformation, Park's transformation etc. Park's transformation applied to three-phase currents is shown below in matrix form:

$$\boldsymbol{I_{dqo} = TI_{abc} = \frac{2}{3}\begin{bmatrix} \cos\theta & \cos\left(\theta - \frac{2\pi}{3}\right) & \cos\left(\theta + \frac{2\pi}{3}\right) \\ -\sin\theta & -\sin(\theta - \frac{2\pi}{3}) & -\sin(\theta + \frac{2\pi}{3}) \\ \frac{1}{2} & \frac{1}{2} & \frac{1}{2} \end{bmatrix}\begin{bmatrix} I_a \\ I_b \\ I_c \end{bmatrix}} \qquad (2.1)$$

The inverse transform is:

$$\boldsymbol{I_{abc} = Te^{-1}I_{dqo}} = \begin{bmatrix} \boldsymbol{\cos\theta} & \boldsymbol{-\sin\theta} & \boldsymbol{1} \\ \boldsymbol{\cos\left(\theta - \frac{2\pi}{3}\right)} & \boldsymbol{-\sin(\theta - \frac{2\pi}{3})} & \boldsymbol{1} \\ \boldsymbol{\cos\left(\theta + \frac{2\pi}{3}\right)} & \boldsymbol{-\sin(\theta + \frac{2\pi}{3})} & \boldsymbol{1} \end{bmatrix} \begin{bmatrix} \boldsymbol{I_d} \\ \boldsymbol{I_q} \\ \boldsymbol{I_o} \end{bmatrix} \quad (2.2)$$

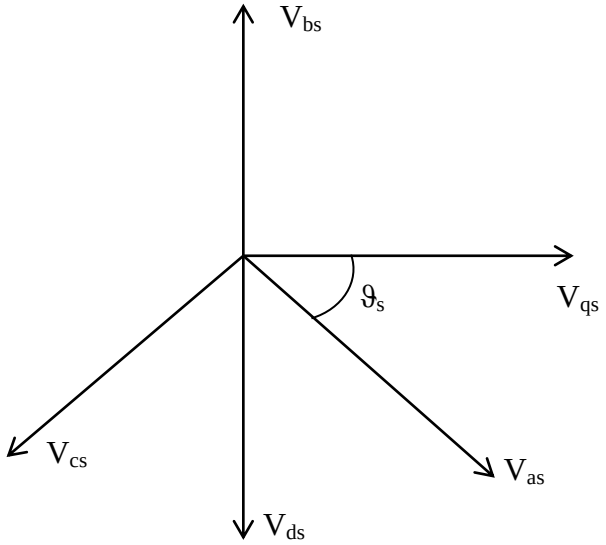

Fig. 2.3 abc-dq axes transformation in synchronously rotating frame of reference

A simple abc- dq representation in a synchronously rotating reference frame is shown in Fig. 2.3. The figure shows the three phase stator voltages V_{as}, V_{bs} and V_{cs} displaced 120^0 apart in space and also the two resolved voltages V_{qs} and V_{ds} perpendicular to each other. In this frame of reference, the reference frame is rotating at speed ω_s (ϑ_st).

The various parameters are calculated as under:

Voltage equations are:

$$\boldsymbol{V_{qs} = R_s * i_{qs} + \frac{d\Psi_{qs}}{dt} + \omega_e \Psi_{ds}} \quad (2.3)$$

$$\boldsymbol{V_{ds} = R_s * i_{ds} + \frac{d\Psi_{ds}}{dt} - \omega_e \Psi_{qs}} \quad (2.4)$$

$$\boldsymbol{V_{qr} = R_r * i_{qr} + \frac{d\Psi_{qr}}{dt} + (\omega_e - \omega_r)\Psi_{dr}} \quad (2.5)$$

$$\boldsymbol{V_{dr} = R_r * i_{dr} + \frac{d\Psi_{dr}}{dt} - (\omega_e - \omega_r)\Psi_{qr}} \quad (2.6)$$

Flux equations are:

$$\Psi_{qs} = \boldsymbol{L_{ls} * i_{qs} + (i_{qs} + i_{qr})L_m} \quad (2.7)$$

$$\Psi_{qr} = \boldsymbol{L_{lr} * i_{qr} + (i_{qs} + i_{qr})L_m} \quad (2.8)$$

$$\Psi_{ds} = \boldsymbol{L_{ls} * i_{ds} + (i_{ds} + i_{dr})L_m} \quad (2.9)$$

$$\Psi_{dr} = \boldsymbol{L_{lr} * i_{dr} + (i_{ds} + i_{dr})L_m} \quad (2.10)$$

Where V_{qs} & V_{ds} are the applied voltages to the stator; i_{ds}, i_{qs}, i_{dr}, & i_{qr} are the corresponding d & q axis currents; Ψ_{qs}, Ψ_{qr}, Ψ_{ds} & Ψ_{dr} are the rotor & stator flux component; R_s, R_r are the stator & rotor resistances; L_{ls} & L_{lr} denotes the stator & rotor leakage inductances, whereas Lm is the mutual inductance.

2.4 Theory of Vector Control

2.4.1 Principle of Vector Control

The principle behind the Vector control is to control the Induction motor in a similar fashion to that of a separately excited DC motor. The advantage of DC motor is that it has an inherent decoupling present between the flux and torque. This inherent decoupling allows the control of separately excited DC motor in a simple and more efficient manner. The torque and flux, in case of the DC motor are controlled by the armature and field currents respectively. The same principle can be implemented in case of an induction motor also to control the torque and flux independently, which is possible through proper transformation.

A Separately excited DC motor is shown in Fig. 2.4. In a dc machine, neglecting the armature reaction effect and field saturation, the developed torque is given by

$$T_e = K_t \Psi_f \Psi_a = K_t' I_f I_a \quad (2.11)$$

Where, I_a = armature current

& I_f = field current

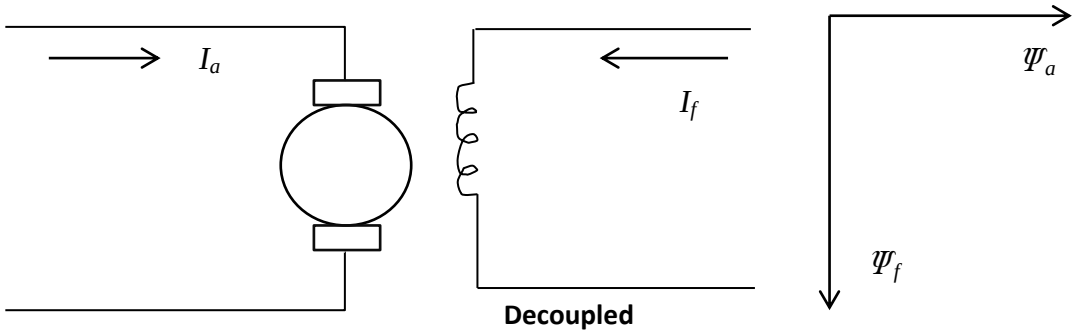

Fig. 2.4 Separately excited DC motor

In case of a DC machine, the field current I_f produces field flux Ψ_f, and the armature current I_a produces armature flux Ψ_a. The construction of the machine is such that these two flux vectors are perpendicular to each other. Due to this orthoganility, the two flux vectors are independent of each other and each can be controlled independently. This allows the control of torque by controlling the armature current and the flux by controlling the field current without each affecting one another.

Ideally a vector controlled induction motor can be controlled in a same manner as that of a separately excited DC motor. This is done by means of transformation of the three-phase AC parameters (i_a, i_b, i_c) to two DC quantities (i_d, i_q).

With vector control, i_d is analogous to field current I_f and i_q is analogous to armature current I_a of a dc machine. Therefore, the torque can be expressed as

$$T_e = K_t \Psi_r I_q = K_t' I_q I_d \quad (2.12)$$

Where Ψ_r = absolute peak value of the sinusoidal space vector. This dc machine like performance is only possible if *'i_d' is* oriented in the direction of Ψ_r and 'i_q' is established perpendicular to it. This means that when i_q^* is controlled; it affects the actual i_q current

only, but does not affect the flux Ψ_r. Similarly, when i_d* is controlled, it controls the flux only and does not affect the I_q component of current [67]. This vector or field orientation of current is essential under all operating condition in a vector control drive.

In the '*dq'* reference frame, the electromagnetic torque equation is given by

$$\boldsymbol{T_e} = \frac{\boldsymbol{3 * P * L_m}}{\boldsymbol{2 * 2 * L_r}} * \left(\Psi_{\boldsymbol{dr}} \boldsymbol{i_{qs}} - \Psi_{\boldsymbol{qr}} \boldsymbol{i_{ds}}\right) \tag{2.13}$$

Where *P* denotes the pole number of the motor

2.4.2 Synchronously Rotating Reference Frame

In a vector control strategy, the *d*-*q* frame rotates along with the rotor flux (which is maintained at its rated value). The *d*-axis is aligned with the direction of the rotor flux. Therefore, the d-axis component of the rotor flux is null and the expression of the electromagnetic torque simplifies as follows

$$\boldsymbol{T_e} = \frac{\boldsymbol{3 * P * L_m}}{\boldsymbol{2 * 2 * L_r}} * (\Psi_{\boldsymbol{dr}} \boldsymbol{i_{qs}}) \tag{2.14}$$

Then the electromagnetic torque is controlled only by q-axis stator current.

The rotor magnetizing current can be expressed in terms of the d-axis stator current as follows:

$$\boldsymbol{i_{mr}} + \boldsymbol{T_r} \frac{\boldsymbol{di_{mr}}}{\boldsymbol{dt}} = \boldsymbol{i_{ds}} \tag{2.15}$$

Where, 'T_r' is the rotor time constant.

$$\boldsymbol{T_r} = \frac{\boldsymbol{L_r}}{\boldsymbol{R_r}} \tag{2.16}$$

A stationery frame to synchronously rotating reference frame conversion is shown in Fig. 2.5, with all equations of conversion shown in the figure.

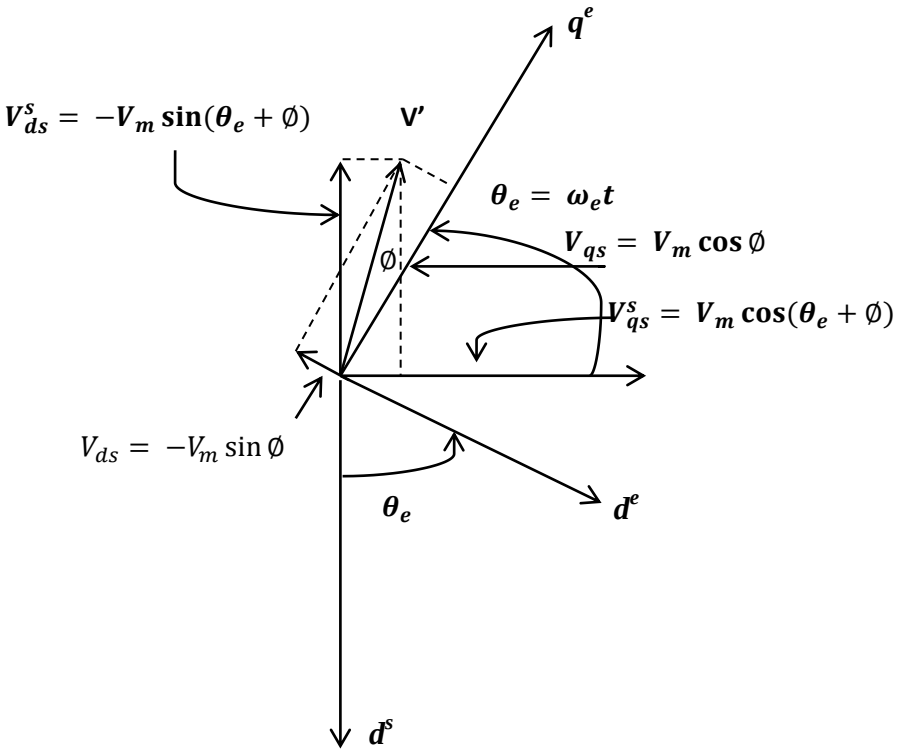

Fig. 2.5 Stationary frame to synchronously rotating frame transformation

Thus the *d*-axis stator current (i_{ds}) is controlled to maintain the flux at its rated value whereas the *q*-axis stator current (i_{qs}) is varied to achieve the desired electromagnetic torque. Therefore, the IM can be controlled just like a separately excited dc motor drive because the *d*- and *q*-axes are orthogonal.

2.5 Types of Vector Control

There are two different methods of vector control method, besides others. These two methods are Direct Vector Control & Indirect Vector Control. The two methods are different based upon the principle of generation of the control vector "theta (ϑ)". It should be mentioned here that the orientation of 'i_{ds}' with rotor flux, air gap flux, or stator flux is possible in vector control. However, rotor flux orientation gives natural decoupling control, whereas air gap or stator flux orientation gives a coupling effect which has to be compensated by a decoupling compensation current [67]. The two methods are described in the following section.

2.5.1 Direct Vector Control

In direct vector control the flux vector is either measured or estimated, and the angle obtained is used for the coordinate transform of the stator current space phasor. With the flux vector available, the torque can be calculated. In case of direct vector control the control vector is measured directly using voltage & current measurement algorithms. Rotor flux phasor position θ_f is to be obtained given by

$$\boldsymbol{\theta_f = \int \omega_s \, dt} \tag{2.17}$$

The general block diagram of a direct vector control scheme is shown in Fig. 2.6.

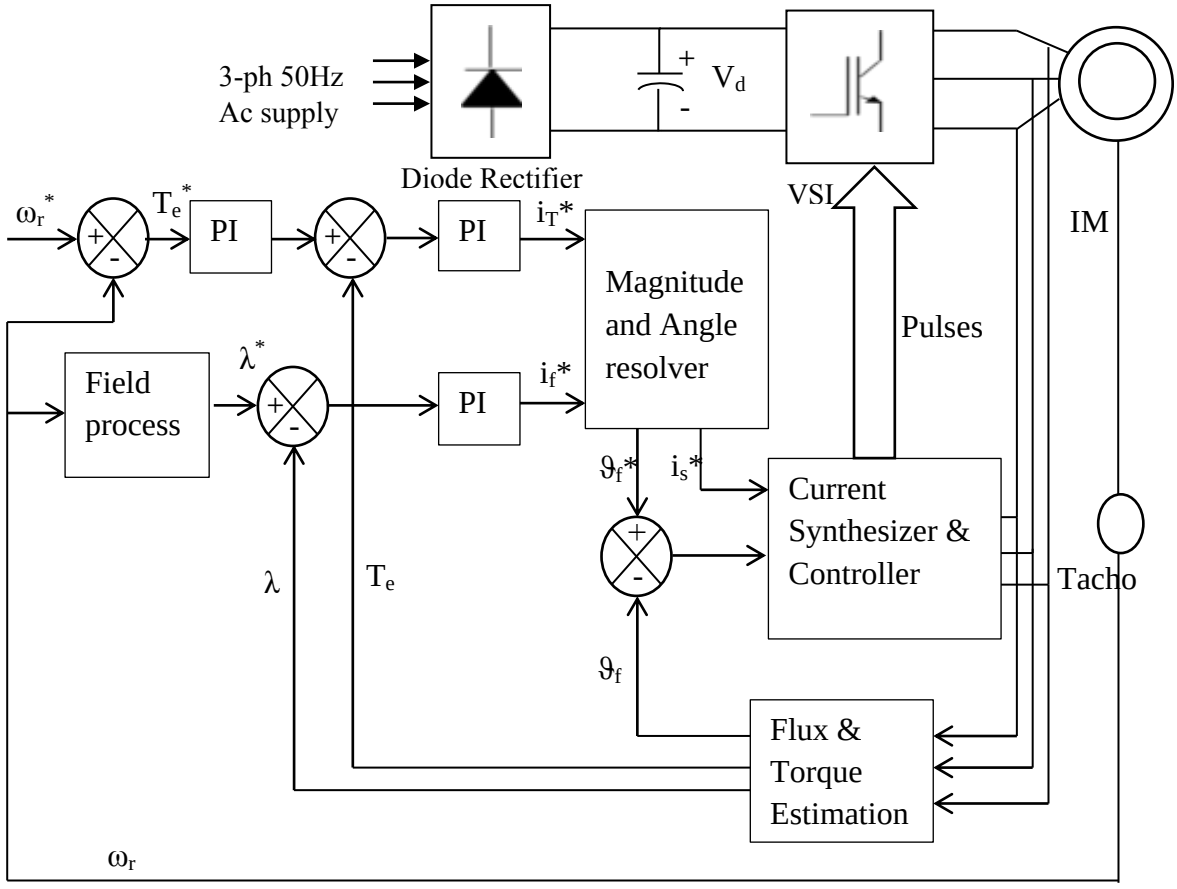

Fig. 2.6 Block diagram representing direct vector control scheme

The system inherits a considerable complexity and the control system depends on all motor parameters. In the direct method, also known as flux feedback method, the airgap flux is directly measured with the help of sensors such as Hall probes, search coils or tapped stator windings or estimated/observed from machine terminal variables such as stator voltage, current and speed. A major drawback with the direct orientation schemes is their inherent problem at very low speeds when the machine IR drop dominates and the required integration of the signals to measure the airgap flux is difficult.

The estimation of flux in direct vector control strategy has been proposed by many. There are essentially two main models of flux estimation [67].

1. Voltage model: In this method, the machine terminal voltages and currents are sensed and the fluxes are computed from the stationary frame equivalent circuit. This model is generally good for high speed regions only.
2. Current model: In the low-speed region, the rotor flux components can be synthesized more easily with the help of speed and current signals.

2.5.2 Indirect Vector Control

In case of Indirect Vector Control, the rotor angle θ_e is generated in an indirect manner using the measured speed ω_r and the slip speed ω_{sl}.

$$\boldsymbol{\theta_e = \int \omega_e dt = \int (\omega_r + \omega_{sl}) dt = \theta_r + \theta_{sl}} \tag{2.18}$$

The speed error, with the help of a PI controller or any other intelligent controller, is converted into a torque controlling current component i_{qs}^*, of the stator current.

This current component is used to regulate the torque along with the slip speed.

A general block diagram showing an indirect vector control scheme is shown in Fig. 2.7

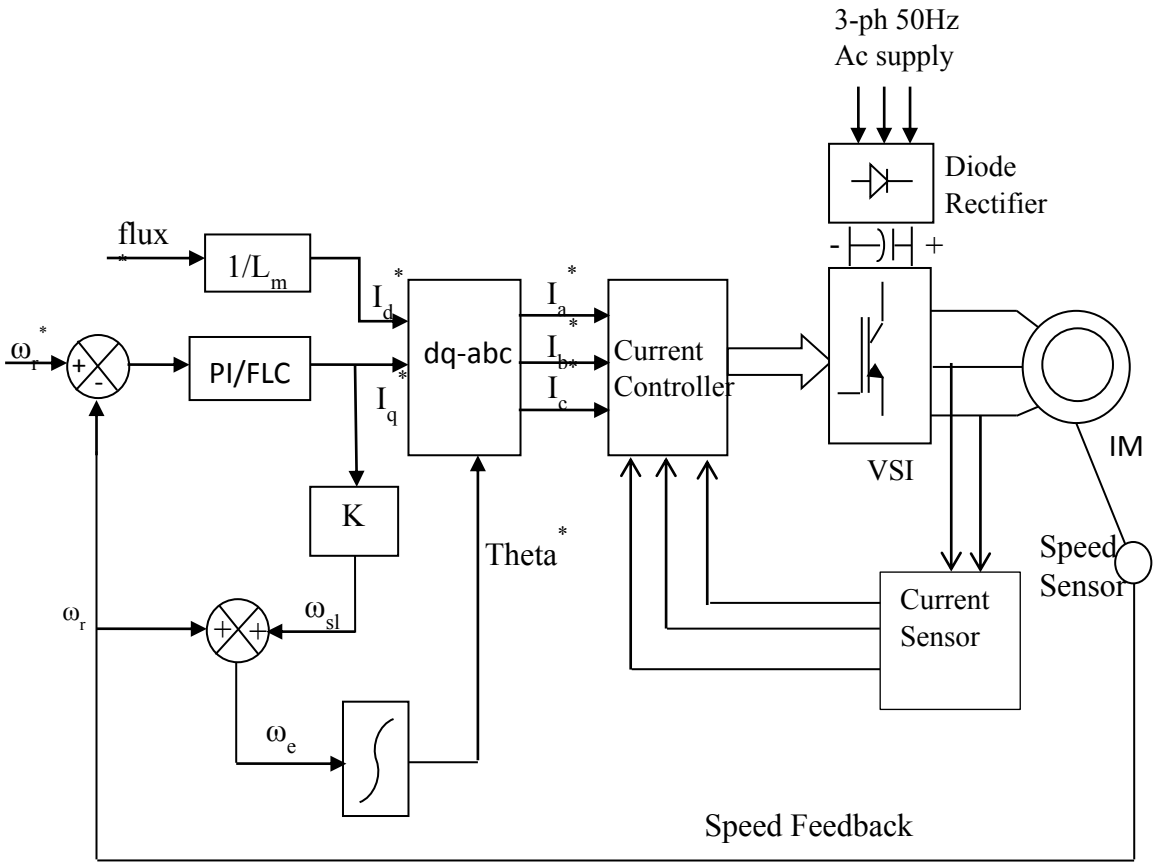

Fig. 2.7 Block Diagram representing Indirect Vector Control Scheme

2.5.3 Comparison between Indirect & Direct Vector Control

I. Indirect VC involves feed-forward generation of unit vector signals while as Direct VC involves feedback mechanism.

II. The direct method accomplishes commutation with electrical or magnetic feedback from the motor while the indirect method accomplishes commutation with velocity feedback from the motor and a feed forward slip command.

III. Both schemes typically utilize some type of stator current regulation.

IV. The velocity signal is generally a cleaner control signal than the voltage from a PWM inverter; thus, control is inherently more robust with the indirect method.

V. The significant difference between Vector control and others is that the developed motor model and outputs are based on the fundamental operating condition of the motor and not some unrelated signals. In other words, it is based on fundamental component terminal voltages and currents of the motor.

VI. While the direct method is inherently the most desirable control scheme, it suffers from high cost and the unreliability of the flux measurement.

2.6 Conclusion

In this chapter, the dynamic d-q model of three-phase induction motor in synchronously rotating reference frame and stationary reference frame have been discussed. The state-space equations in terms of flux linkages were derived mainly for simulation study.

The frequency of the drive is not directly controlled as in scalar control. The machine is essentially "self-controlled," where the frequency as well as the phase is controlled indirectly with the help of the unit vector. The transient response of induction motor will be fast and dc machine-like because torque control by i_{qs} does not affect the flux. Like a dc machine, speed control is possible in four quadrants without any additional control elements (like phase sequence reversing). In forward motoring condition, if the torque is negative, the drive initially goes into regenerative braking mode, which slows down the speed. At zero speed, the phase sequence of the unit vector automatically reverses, giving reverse motoring operation. In both the direct and indirect vector control methods the instantaneous current control of the inverter is necessary.

Chapter III

Hardware Implementation of Indirect Vector Controlled Induction Motor

3.1 Introduction

In this chapter, the description of the hardware components used in the project and the complete control scheme of indirect vector control are presented. The general block diagram of the complete hardware scheme is given in Fig. 3.1.

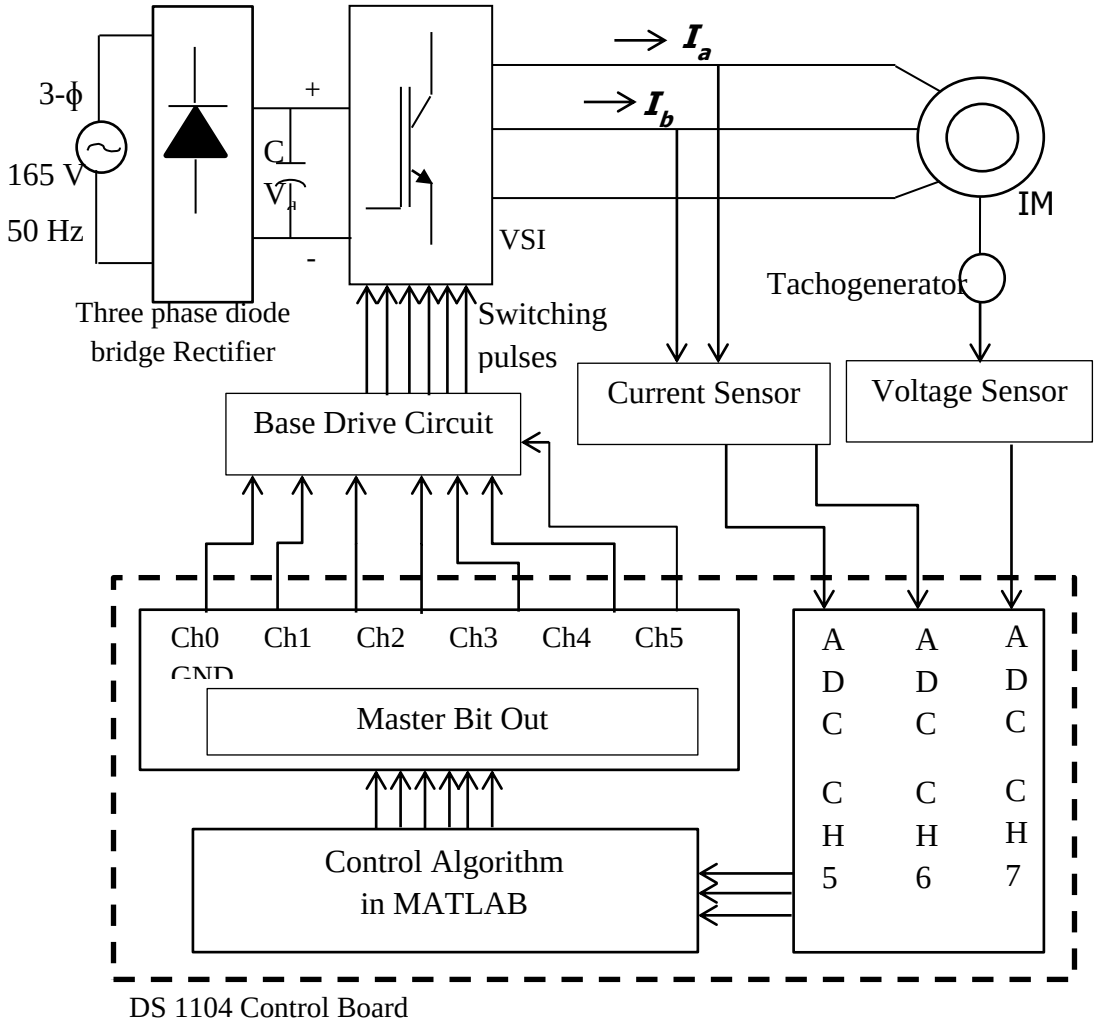

Fig. 3.1 Block Diagram of the complete hardware scheme

3.2 Description of Vector Controlled Induction Motor

As shown in Fig. 3.1, the main components used in the hardware scheme are

1. Voltage Source Converter (VSC)
2. Sensors
3. DS-1104 Control Board

3.2.1 Voltage Source Converter

A converter is a term coined in general for a rectifier or an inverter. A rectifier converts AC voltage into DC voltage while as an inverter converts DC voltage into AC voltage.

A three phase Voltage Source Inverter (VSI) is used in the hardware implementation of the scheme, manufactured by the Semikron Industries. The Voltage source converter consists of a three phase diode bridge rectifier which converts AC voltage into DC voltage and the VSI consists of three phase IGBT bridge inverter. The VSC consists of capacitors to filter the DC link voltage.

In the VSI, IGBT semiconductor switches are used. IGBT offers advantages over other semiconductor switches. The IGBT is suitable for many applications in power electronics, especially in Pulse Width Modulated (PWM) servo and three-phase drives requiring high dynamic range control and low noise. IGBT improves dynamic performance and efficiency and reduces the level of audible noise. It is equally suitable in resonant-mode converter circuits. Optimized IGBT is available for both low conduction loss and low switching loss. It has a very low on-state voltage drop. It can be easily controlled in high voltage and high current applications.

The rectifier circuit works in the ratio of 1:1.35 i.e. for an input ac voltage of 100 V, the rectifier output is a 135 V dc voltage. The pulses to the inverter are PWM pulses generated from the MATLAB model using a Hysteresis current controller and fed to the inverter through DS-1104 isolated using an optocoupler circuit.

A block diagram showing the IGBT based VSC is shown in Fig. 3.2.

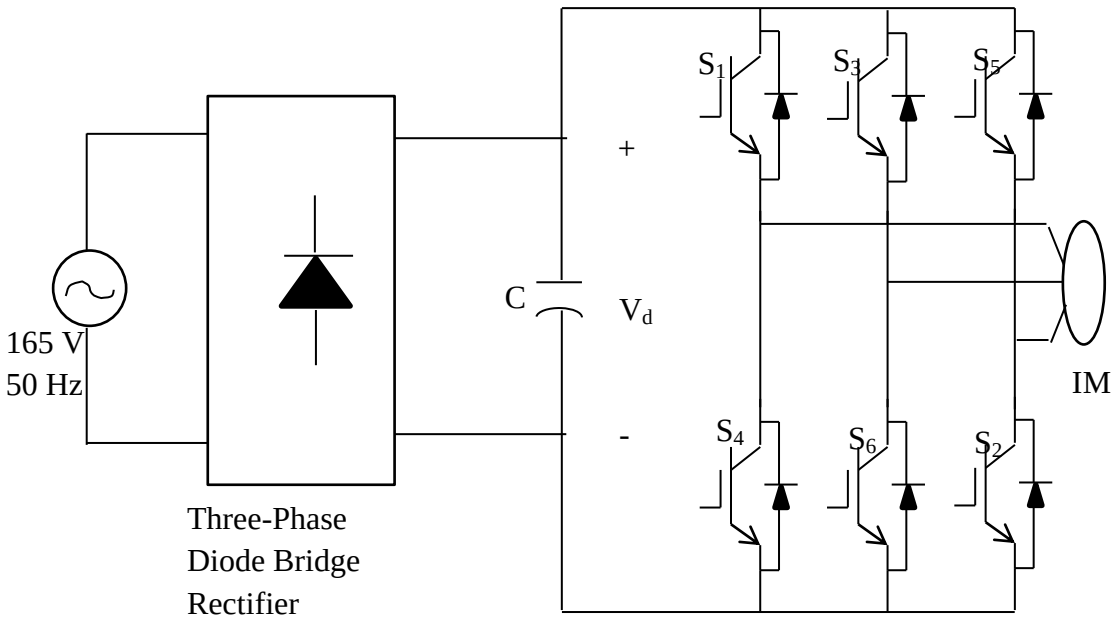

Fig. 3.2 Voltage Source Converter (IGBT based)

3.2.2 Sensors

A sensor is a converter that measures a physical quantity and converts it into a signal which can be read by an observer or by an (today mostly electronic) instrument. ABB voltage & ABB current sensors are being used in the project.

A current sensor is a device that detects electrical current (AC or DC) in a wire, and generates a signal proportional to it. The generated signal could be analog voltage or current or even digital output. It can be then utilized to display the measured current in an ammeter or can be stored for further analysis in a data acquisition system or can be utilized for control purpose.

The voltage sensor is used to sense the voltage from the tachogenerator (speed sensor). The relative value of voltage is traced to find out the value of speed. ABB current sensors are based on Hall Effect technology. They allow for the measurement of direct, alternating and impulse currents, with galvanic insulation between the primary & secondary circuits. The primary current flowing across the sensor produces primary magnetic flux. The Hall probe in the air gap provides a voltage proportional to this flux.

The electronic circuit amplifies this voltage and converts it into secondary current which multiplied by the number of turns of secondary winding cancels out the primary magnetic flux. The current sensor is used to sense the current in any two phases and the third current is estimated using the two currents.

The ABB voltage sensor used is in the project is EM010-9237.

The ABB current sensors used are EH050AP.

The detailed specification of the ABB voltage and current sensors are given in Appendix C.

3.2.3 DS1104 Control Board

The DS1104 R&D Controller Board upgrades the PC to a development system for rapid control prototyping (RCP) [69]. The real-time hardware, based on a PowerPC microprocessor and its I/O interfaces make the board ideally suited for developing controllers in various fields, in both industry and academics. The DS1104 R&D Controller Board is a standard board that can be plugged into a PCI (Peripheral Component Interconnect) slot of a PC. The DS1104 is specifically designed for the development of high-speed multivariable digital controllers and real-time simulations in various fields. It is a complete real-time control system based on a 603 PowerPC floating-point processor running at 250 MHz. For advanced I/O purposes, the board includes a slave-DSP subsystem based on the TMS320F240 DSP microcontroller [70, 71].

Interfacing of DS1104 & PC- MATLAB is done in order to ease the operation of control. The three-phase current and speed once sensed are fed to the ADC port of DS1104 by means of BNC cable. DS1104 interfaces with the MATLAB, where the control circuit is designed. The gate pulses are determined through the control circuitry. These gate pulses are then fed to the inverter through the Digital I/O connector port of DS1104 separated by the isolating circuit in order to prevent the gate from being shorted. The pulses determine the speed of the induction motor.

The DS1104 contains two different types of analog/digital converters (ADCs) for the analog input channels:

■ One 16-bit ADC with four multiplexed input signals: the channels, ADCH1 ... ADCH4

■ Four 12-bit parallel ADCs with one input signal each: the channels, ADCH5 ... ADCH8

The digital I/O connector (CP17) is a 37-pin, male Sub-D connector located on the front of the connector panel [70].

The important thing to note is that the ADC input to the DS-1104 should be between ±10 V. In order to make this possible, the gain of current sensor and voltage sensor are accordingly set in the circuit.

The technical details of DS-1104 are given in Appendix D.

3.3 Experimental Setup

The hardware setup is shown in Fig. 3.3. The current sensor senses the line current i_a and i_b from the motor. The third current i_c is obtained from numerical computation. The voltage sensor is meant to sense the voltage from the Tacho-generator, which is actually the speed equivalent. These sensed current and voltage signals are fed to the ADC terminals of the D-space controller, from where it goes to the MATLAB/Control Desk. The DS-1104 by default divides the voltage signal at the input of ADC by a factor of ten. This gain has to be multiplied to the current signal and voltage signal inside the MATLAB model. In the MATLAB the control scheme is implemented using proper '*RTI'* block sets provided for interfacing MATLAB with DS-1104. Proper gain values of current sensor and voltage sensor are implemented within the MATLAB model to avoid malfunctioning of the Control scheme. The pulses are generated from the MATLAB/Simulink model, which are fed to the inverter through the Digital I/O connector port of the D-space controller. The Control Desk, which is software platform of DS-1104, helps in online tuning of parameters of PI and FLC, for providing efficient control of the motor speed and current.

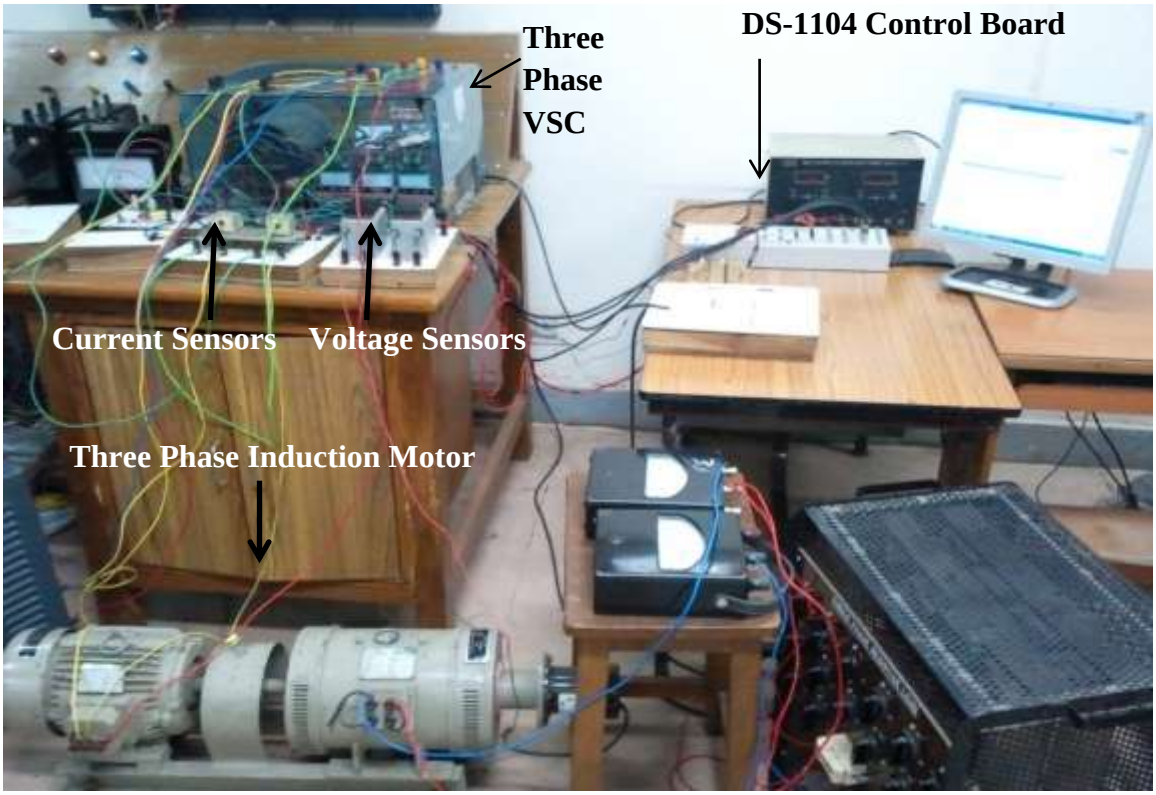

Fig. 3.3 Hardware setup for indirect vector control drive for 3 Hp, 230 V, 1440 rpm IM

The actual control station of the whole scheme lies inside the MATLAB/Simulink model. The operation of the scheme is based on the working of vector control. The speed controllers used in the scheme are PI controller and Fuzzy Logic Controller (FLC). The two controllers are individually used to control the speed of the motor and the results so obtained from them are matched to check the performance of the two controllers.

3.3.1 Operation with PI

PI controller is a conventional control technique used in most of the control process applications. The PI controller is used as a speed controller in this scheme. The input of the PI controller is the difference between the reference speed ω* and the actual measured speed ω_r. The output and input relationship of a PI speed controller is described as

$$\boldsymbol{e_o = K_p(e) + K_i \int e\,dt} \qquad (3.1)$$

where, $e = \omega^* - \omega_r$

The PI controller is designed in the MATLAB shown in Fig. 3.4. Saturation control link is meant to limit the output amplitude.

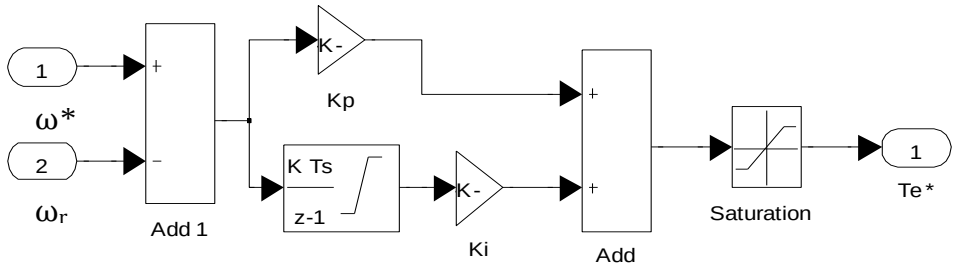

Fig.3.4 Proportional Integral Controller block diagram

The PI controller can be tuned using any method available to find out the best possible values of K_p & K_i. There are tuning methods like Ziegler-Nichols method, Cohen-Coon method etc. used for tuning PI controller. The optimum values of the parameters K_p and K_i decides the performance of the PI speed controller.

3.3.2 Operation with FLC

3.3.2.1 Fuzzy Logic Controller:

Fuzzy logic is a branch of artificial intelligence that deals with reasoning algorithms used to emulate human thinking and decision making in machines. These algorithms are used in applications where process data cannot be represented in binary form. Fuzzy logic requires prior knowledge in order to reason. This knowledge is provided by a person who knows the process or machine (the expert). This knowledge is stored in the fuzzy system. The FLC general scheme is shown in Fig. 3.5 in which the error & rate of change of error is fed to FLC to control the speed of induction motor. The error is the difference of actual speed from the reference speed. The control of torque is done by controlling the i_q component of stator current. From the FLC we get a controlled output of current i_q, which is then fed to the Hysteresis current controller to generate gating pulses for the voltage source inverter.

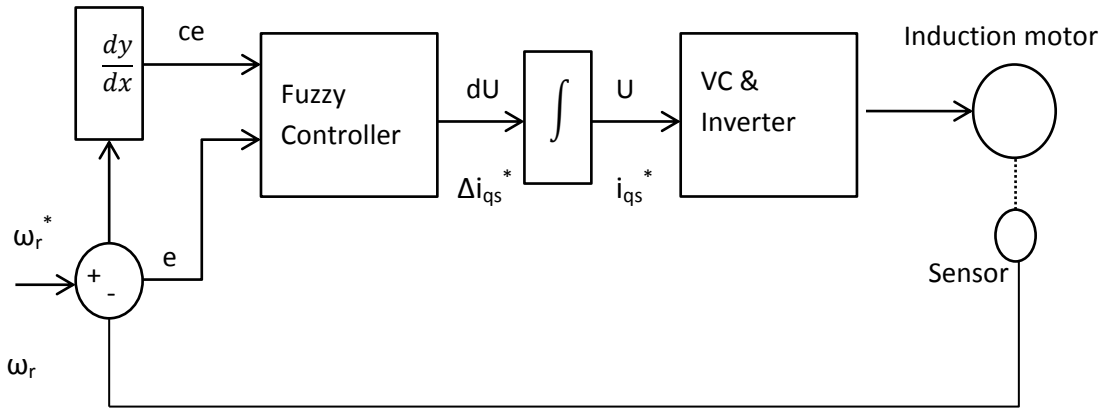

Fig. 3.5 Functional block diagram of Fuzzy Logic Controller

Here the first input is the speed error 'e' and second is the change in speed error '*ce'* at sampling time 't_s'. The two input variables *e (ts)* and *ce (ts)* are calculated at every sampling time as

$$\boldsymbol{e(t_s) = \omega_r^*(t_s) - \omega_r(t_s)} \quad (3.2)$$

$$\boldsymbol{ce(t_s) = e(t_s) - e(t_s - 1)} \quad (3.3)$$

Where '*ce'* denotes the change of error '*e'*, 'ω_r*(t_s)' is the reference rotor speed, 'ω_r (t_s)' is the actual speed, '*e* $(t_s$*-1)'* is the value of error at previous sampling time

The stages of FLC are as follows:

3.3.2.2 Fuzzification

In this stage the crisp variables of input *e* (t_s) and *ce* (t_s) are converted into fuzzy variables. The fuzzification maps the error and change in error to linguistic labels of fuzzy sets. Membership function is associated to each label with triangular shape which consists of two inputs and one output. The proposed controller uses following linguistic labels *NB, NM, NS, ZE, PS, PM, PB.* Each of the inputs and output contain membership function with all these seven linguistics. The proposed membership function has been tested through simulation in MATLAB as well as experimentally.

A Sugeno type Fuzzy Logic Controller has been designed for the control system. The inputs i.e. the error, e and change in error, ce follow the membership function plot as shown in Fig. 3.6.

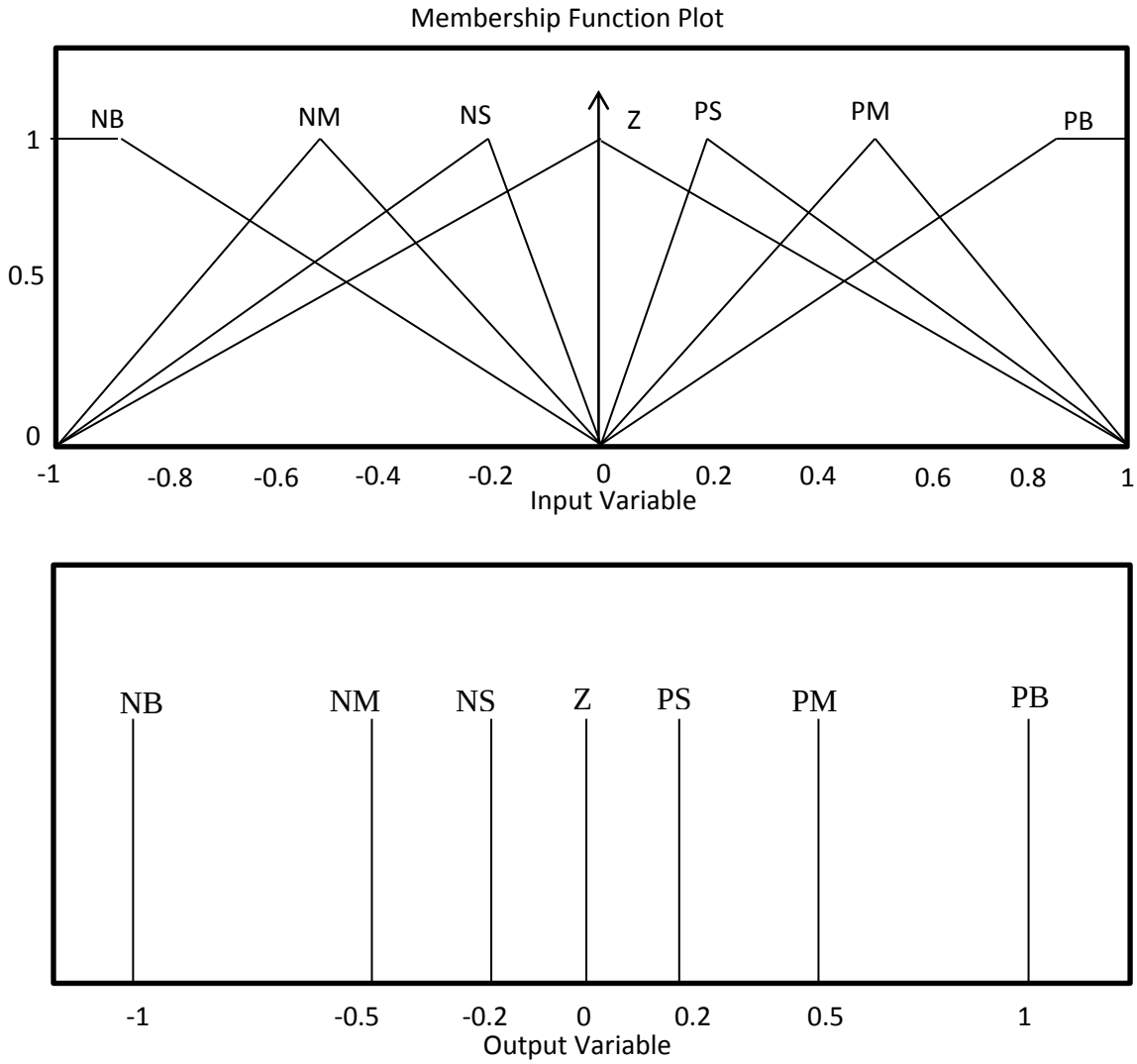

Fig. 3.6 Input and Output membership function representation

3.3.2.3 Rule Base and Inference

Knowledge base involves defining the rules represented as *IF-THEN* rules statements governing the relationship between input and output variables in terms of membership function. In this stage the input variables *e* (t_s) and *ce* (t_s) are processed by the inference mechanism that executes *7*7* rules represented in rule base shown as follows

E / Ce	NB	NM	NS	Z	PS	PM	PB
NB	NB	NB	NB	NB	NM	NS	Z
NM	NB	NB	NB	NM	NS	Z	PS
NS	NB	NB	NM	NS	Z	PS	PM
Z	NB	NM	NS	Z	PS	PM	PB
PS	NM	NS	Z	PS	PM	PB	PB
PM	NS	Z	PS	PM	PB	PB	PB
PB	Z	PS	PM	PB	PB	PB	PB

Table 1: Fuzzy Rule Base

Where various linguistic variables are:

NB Negative Big

NM Negative Medium

NS Negative Small

Z Zero

PS Positive Small

PM Positive Medium

PB Positive Big

Some rules are explained as under

"IF 'e' is NB, AND 'ce' is NB, THEN controller output is NB", i.e. once the error between the reference speed and measured speed is large, and change in error is also large, then the controller also has to act accordingly, i.e. the control output should also be large enough to quickly reduce the error and change in error. This control action will take place initially when the

motor has just started. It can also be observed from the rule base table, that ***"IF 'e' is Z, AND 'ce' is Z, THEN output is Z"***, i.e. since error is zero and is not changing, the controller need not to act and hence the controller output is also zero. This control action can be seen once steady state has been achieved and the speed has set to reference speed.

3.3.2.4 Defuzzification

This stage introduces different methods that can be used to produce fuzzy set value for the output fuzzy variable *ΔT*. Here the centre of gravity or centroids method is used to calculate the final fuzzy value *ΔT (ts)*.

3.3.2.5 Tuning Fuzzy Logic Controller

Tuning FLC is most important part of the process. Proper values of gains need to be choosen so that the FLC membership values are properly selected so as to ensure proper functioning of the controller. The FLC shown in Fig. 3.7 can be tuned in a similar way of PI controller where we can find K_p and K_i as follows:

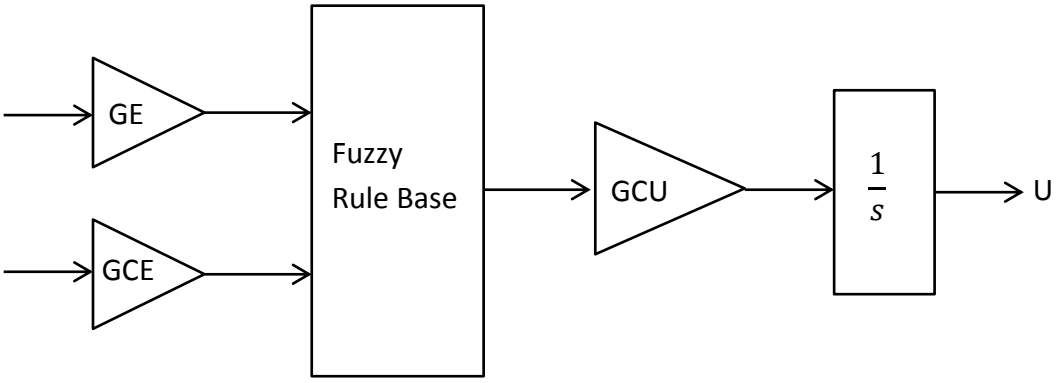

Fig. 3.7 Fuzzy incremental controller

The values are

$$\boldsymbol{GCE * GCU = K_p} \tag{3.4}$$

$$\boldsymbol{\frac{GE}{GCE} = \frac{1}{\tau_i}} \tag{3.5}$$

So now like the PI controller, the parameters *GCE*,*GCU* and *GE* are tuned to find the possible values of K_p & K_i to best fit the values and provide the best control possible through the fuzzy logic controller.

3.4 Conclusion

In this chapter, the hardware components were presented and also the control schemes (PI & FLC) are described. The components were discussed and the ratings of each component are given in the Appendix (A, C and D).

Recent trends show that FLC has proven to be more effective control strategy than PI controller. The Results are presented in the next chapter along with a comparative performance analysis of the two control schemes.

Chapter IV

Simulation and Experimental Results

4.1 Introduction

This chapter presents a detailed simulation study of an indirect vector control Induction motor drive in MATLAB/Simulink. Simulation study of the Indirect Vector Controlled Induction Motor is performed to understand the physical behavior of the drive before actually developing a prototype of Indirect Vector Controlled Induction Motor. The tuning of PI speed controller and FLC controller were carried out through simulation study and the necessary tuning parameters were determined. The performance of Indirect Vector Controlled Induction motor under different operating conditions such as forward and reverse motoring, braking/stopping were analysed through simulation and variation of the motor current, torque and speed were visualized through graphical representation.

4.2 MATLAB Model

Fig. 4.1 shows a MATLAB model of Indirect Vector Controlled Induction motor in Simulink. It comprises of a three-phase Voltage Source Inverter (VSI), a three-phase 3HP, 230V, 1440 rpm Induction Motor, Hysteresis Current Controller, abc – dq conversion block, dq – abc conversion block, flux control element and a torque control element which in turn results in the control of current and speed respectively. The speed controller used in the simulation as shown in Fig. 4.1 (a) is a conventional PI controller. Another control scheme as shown in Fig. 4.1 (b) is a Fuzzy Logic Controller. The FLC is based on the rules described in the previous chapter. The results obtained through simulation are presented later in this chapter for both the control schemes. From Fig. 4.1, it is seen that the current sensed from the Induction motor is decoupled into i_d and i_q component. The flux is controlled by controlling the component i_d of current. The torque is controlled by controlling current i_q, for which speed controllers PI and FLC are implemented. The Hysteresis Current controller is used to generate PWM pulses for the

three-phase VSI. The Hysteresis band determines the switching frequency of the PWM pulses.

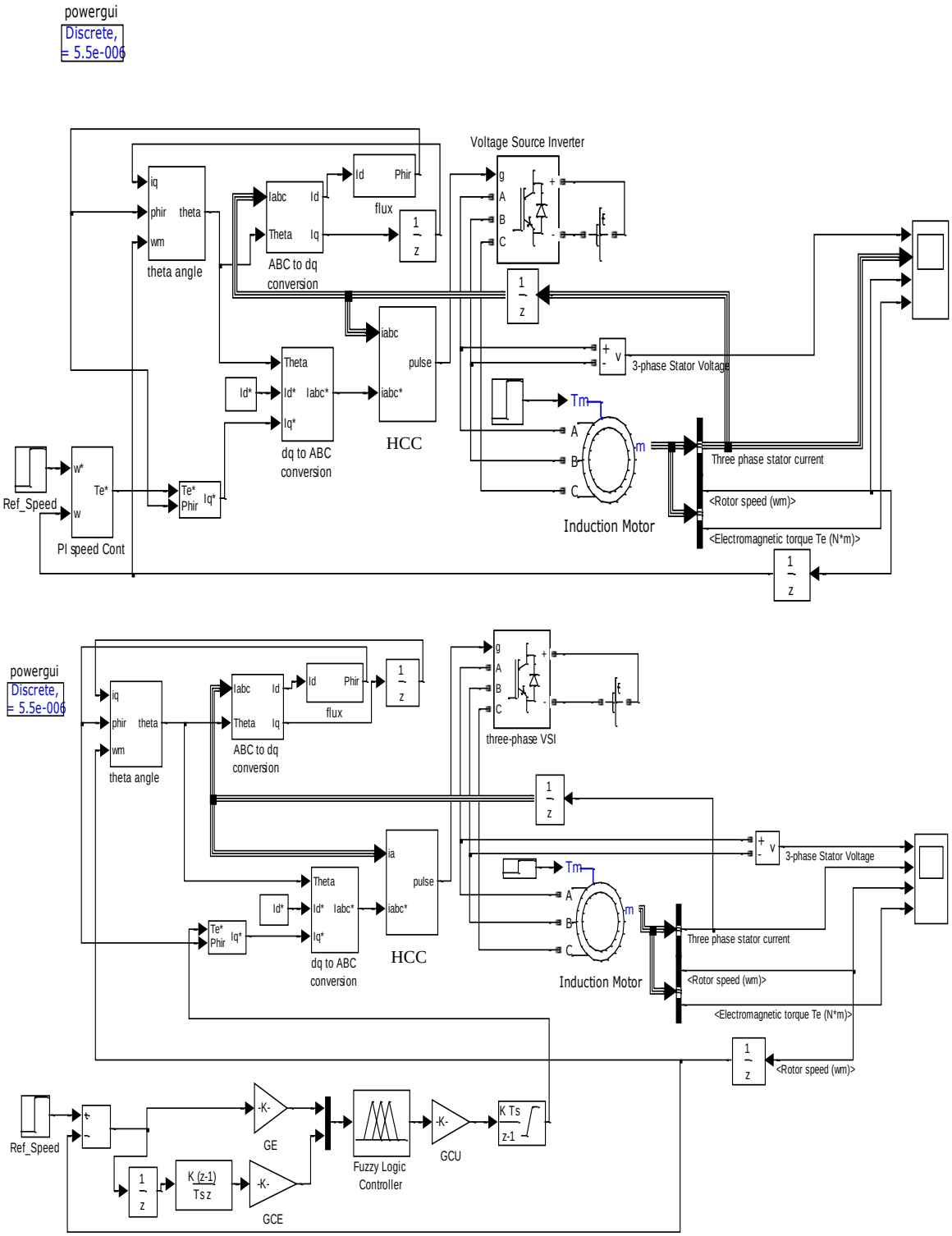

Fig. 4.1 Simulink Model of IVCIM with (a) PI Controller (b) Fuzzy Logic Controller

4.3 Performance Analysis of IVCIM using PI controller

The dynamic behavior of Indirect Vector controlled Induction motor, for a 230 V, 3HP, 1440 rpm (150 rad/sec) Induction Motor, was studied initially through a conventional PI speed controller, where the actual speed (ω_r) of the motor was sensed through a tachogenerator and the output voltage of tachogenerator was sensed through a voltage sensor. For the speed variation in the range of 1210-1440 rpm, the voltage sensor provides a voltage in the range of 68-78 V respectively. The actual speed is compared with voltage corresponding to reference speed ω^* and the difference is processed by PI controller.

In Simulation, initially the motor is run at no load upto t=0.4 sec. After this a load of 9 Nm is applied on the motor. The motor speed is set at a reference speed of 150 rad/sec with a rated rms voltage of 230V.

Fig. 4.2 shows peak to peak line voltage V_{ab}, the line current (i_a, i_b and i_c), the speed (ω) and the electromagnetic torque (T_e) developed by the motor for the above operating conditions. It is observed that the speed transition from zero to rated speed takes place in just over 0.03 sec with an offset of 2 rad/sec. The starting current is initially higher and eventually reduces to steady state at 2.7 Amps.

On application of load of 9 Nm, at t=0.4 sec, there is a momentary dip in speed which is regulated by the PI controller in 0.1 sec and finally the motor settles at 150 rad/sec. During this transition, the current distortion can be observed, which eventually achieves steady state at 8.5 Amps.

The variation of PWM line voltage waveform and torque can also be observed from Fig. 4.2 under different operating conditions using PI controller. The voltage profile shows high frequency switching. Change in modulation can be observed on application of load. The switching is more unipolar when load is applied to the motor.

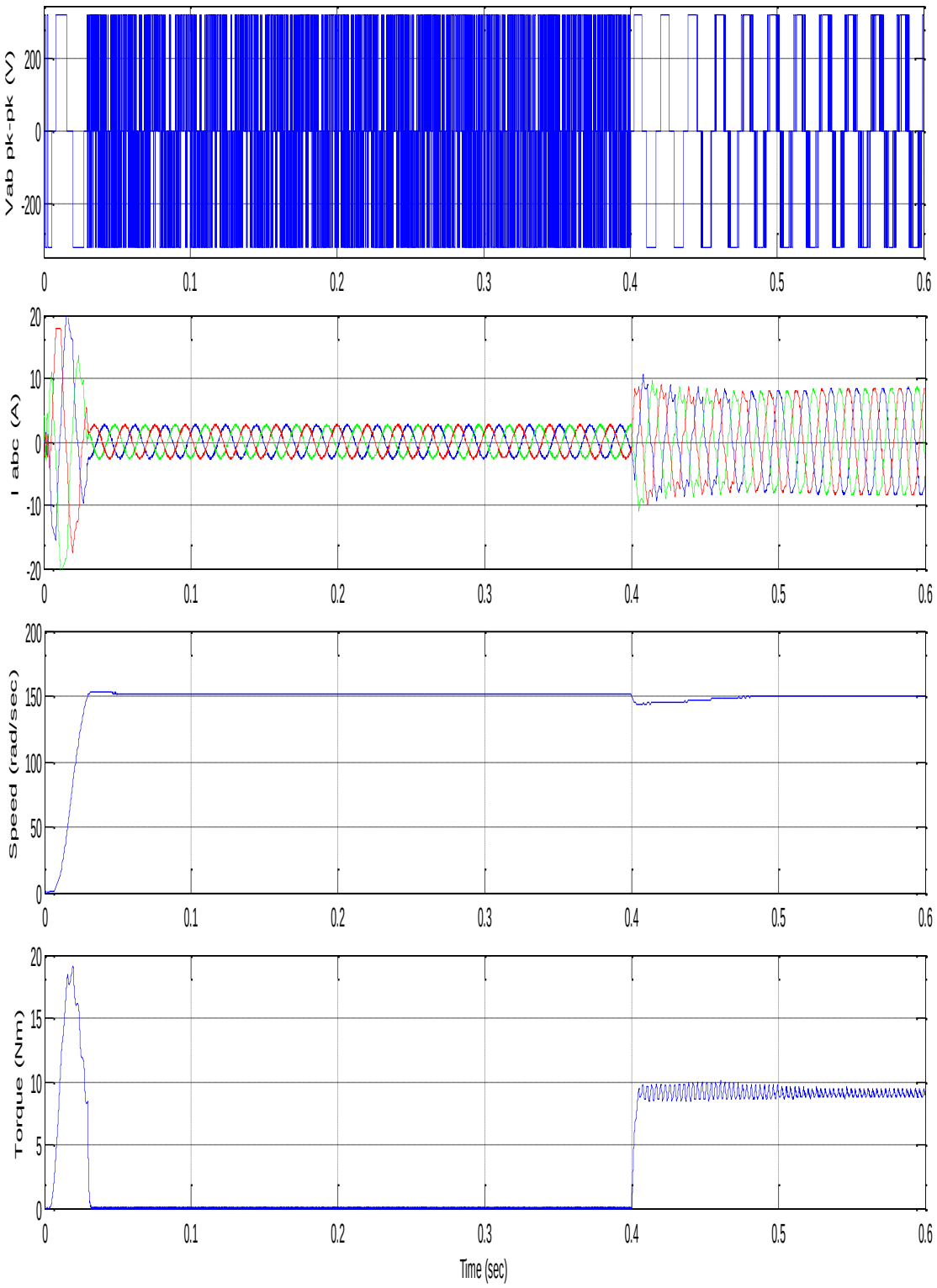

Fig. 4.2 Performance analysis of IVCIM using PI controller for (a) no load (b) load applied at t=0.4 sec

4.4 Performance Analysis of IVCIM using FLC

The dynamic performance of IVCIM is analysed using a Fuzzy Logic Controller also. The FLC speed controller is developed using rule base discussed in the previous chapter. The simulation result is shown in Fig. 4.3. The operating conditions are kept the same as that for the simulation using PI controller to analyse the performance of the two control schemes under same operating conditions.

The performance analysis of IVCIM using FLC is shown in Fig. 4.3. The figure shows peak too peak line voltage V_{ab}, the line current (i_a, i_b and i_c), the speed (ω) and the electromagnetic torque (T_e) developed by the motor for a three-phase, 3HP, 230 V, 1440rpm Induction motor. It is observed that the speed transition from zero to rated speed takes place in 0.03 sec with no offset. The starting current is initially higher and eventually reduces to steady state at 2.7 Amps.

On application of load of 9 Nm, at t=0.4 sec, there is a momentary dip in speed which is recovered in just 0.05 sec and the motor once again settles at the rated speed of 150 rad/sec. During this transition, the current rises slightly above rated, which eventually achieves steady state at 8.5 Amps.

Comparing the graphs obtained from Fig. 4.3 and from Fig. 4.2, it is observed that there is a small time delay, using PI controller, at start for speed transition from zero to the reference speed set for the motor at 150 rad/sec. In case of FLC based controller, the drive shows smoother speed transition and steady state is achieved much quicker than PI based controller. The current profile shows lesser distortion, which means lesser harmonics in case of FLC based IVCIM drive.

The variation of PWM line voltage waveform and torque can also be observed from Fig. 4.3 under different operating conditions using Fuzzy Logic Controller. The torque pulsations in case of FLC based IVCIM are lesser as compared to that of PI based controller.

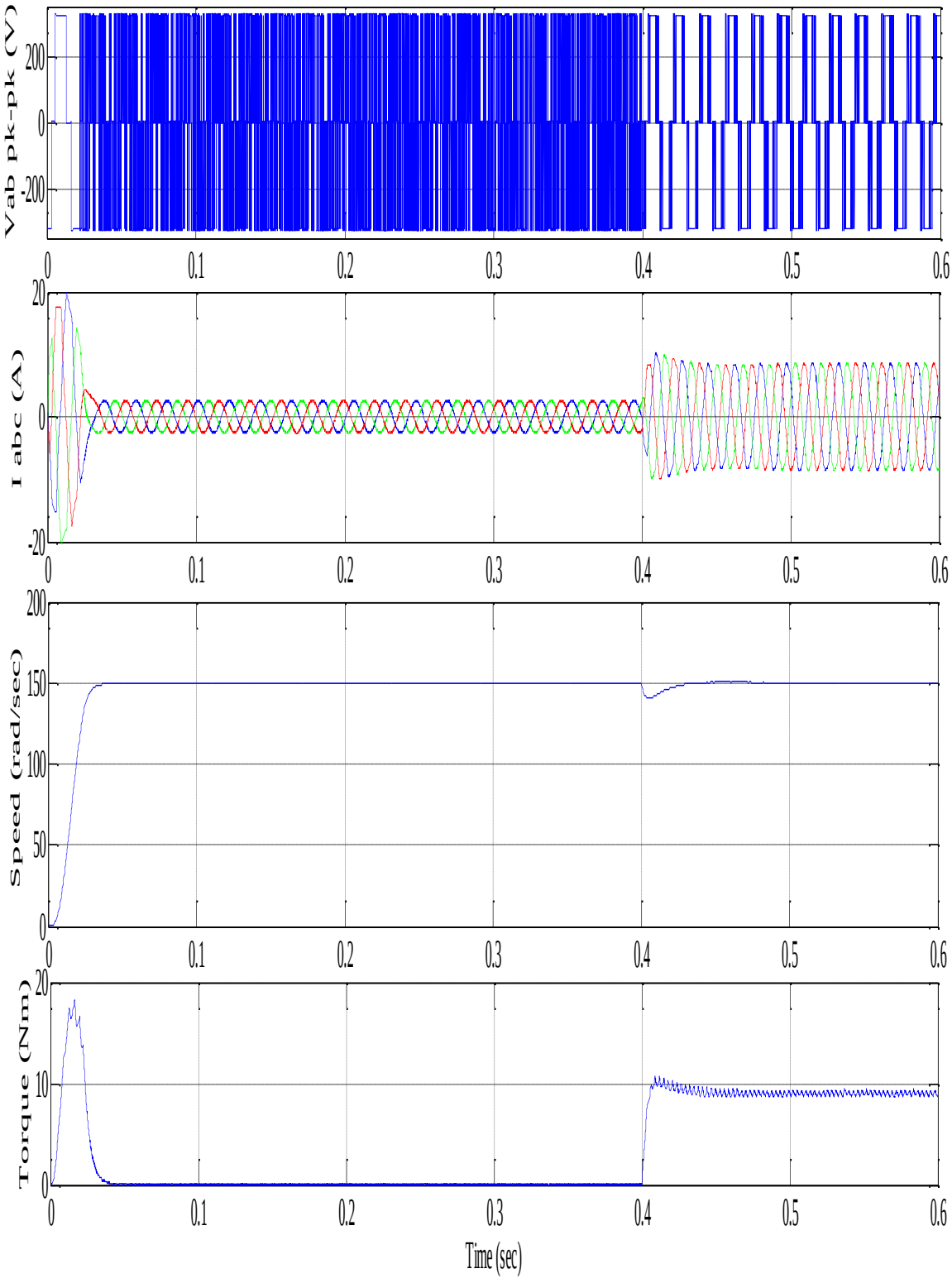

Fig. 4.3 Performance analysis of IVCIM using FLC for (a) no load (b) load applied at t=0.4 sec

4.5 Experimental Results

A complete hardware setup for the 3 HP, 230 V, 1440 rpm Induction motor operated with indirect vector control is implemented and its operation with PI and FLC controller is described to validate the results shown through simulation study. The experimental setup was already presented in Chapter III.

4.5.1 Performance of IVCIM using PI controller

Fig. 4.4 shows the performance of IVCIM using PI controller as obtained experimentally. The figure shows the line current (i_a), the speed (ω) and the electromagnetic torque (T_e) developed by the motor. The Hysteresis band in current controller has been set to 0.1. This determines the switching frequency of the Induction motor.

Initially the Induction motor is made to run at no load. The motor is set to a rated speed of 150 rad/sec. The profile of the motor current as observed from Fig. 4.4 shows high starting current. The performance of the PI controller is experimentally seen to be poor as the motor takes almost 8 sec to reach rated speed. High starting current is seen, but eventually the steady state current of 5 A is reached at no load in 1.5 sec.

At t=10 sec, a load torque of 7 Nm is applied at the motor shaft, which increases the motor current to 7.5 A and also there is a momentary dip in the motor speed. However the PI controller regulates the speed of motor to 150 rad/sec within 2 sec.

The speed transition observed experimentally from Fig. 4.4 is similar to the transition of speed observed through simulation in MATLAB/Simulink as seen in Fig. 4.2. Initially, at no load, it is observed that the speed takes a lot of time to reach steady state. Once load is applied, there is a momentary dip in speed, but the PI controller is able to recover the speed and set it to 150 rad/sec.

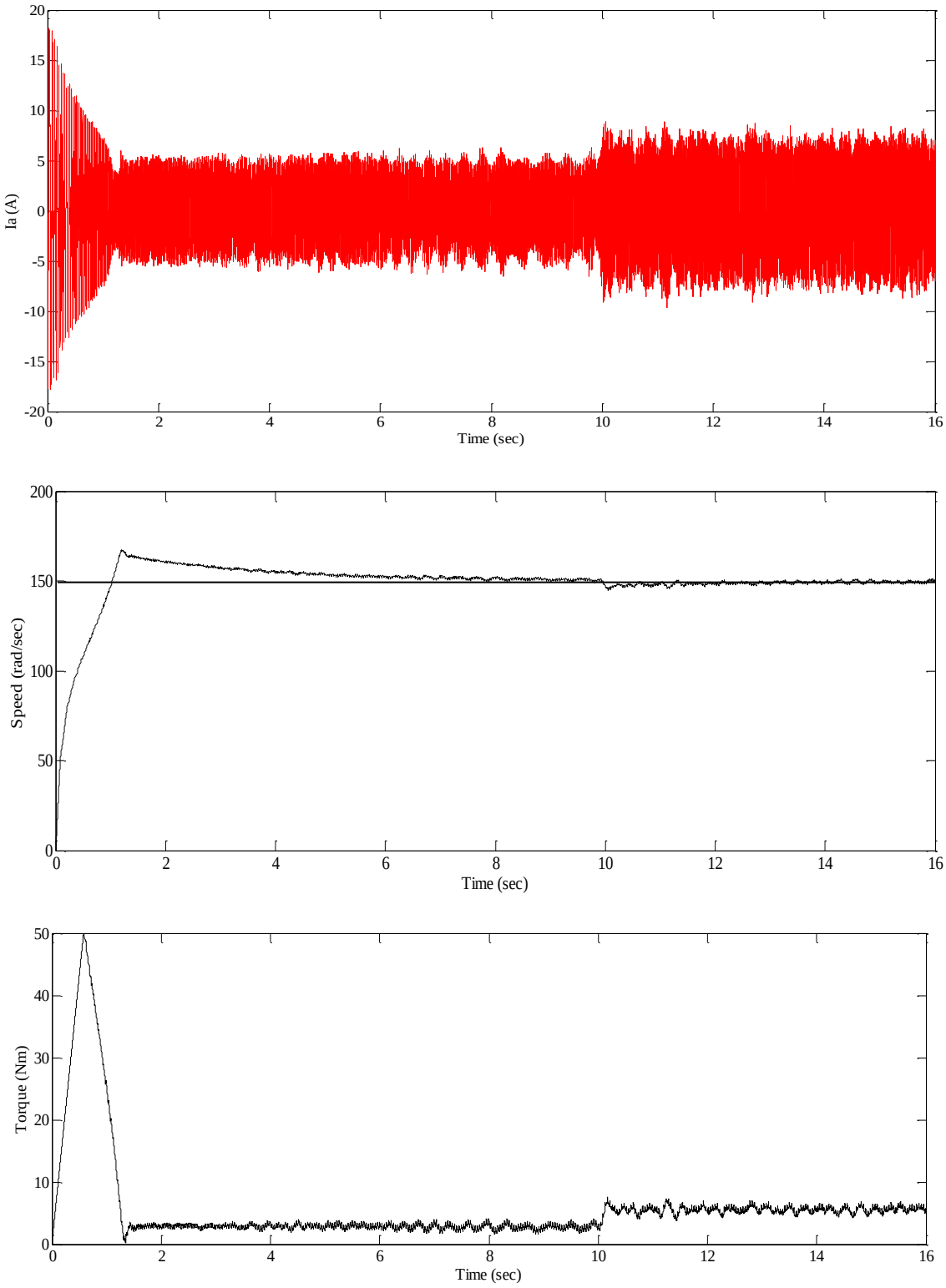

Fig. 4.4 Experimental Performance of IVCIM drive using PI controller

Fig. 4.5 shows steady state value of line currents (i_a, i_b, i_c) at (a) no load (b) load. The effect of Hysteresis current controller can be observed from the current waveform. The motor current is observed at no load and load. The current at no load shows more distortion than the current at load. There are harmonics present at no load due to the non-linear relationship of the magnetising flux and the magnetic field intensity.

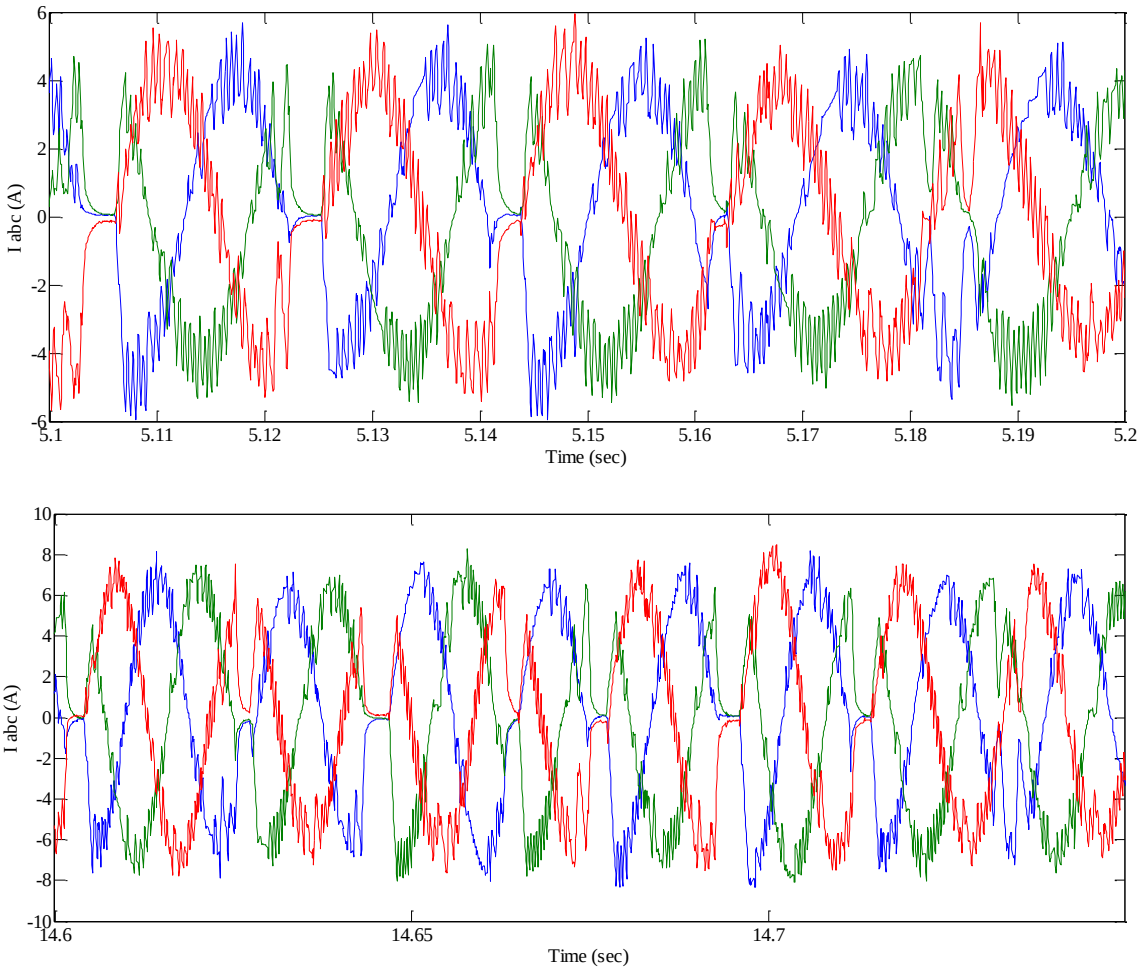

Fig. 4.5 Steady state value of line currents (i_a, i_b, i_c) at (a) no load (b) load

The performance of PI controller in regulating the motor speed in forward, reverse motoring mode and braking mode is shown in Fig. 4.6. The figure shows the line current (i_a), the speed (ω) and the electromagnetic torque (T_e) developed by the motor. The regulation of motor in the three modes is satisfactorily performed by the PI controller. Initially the motor is run in braking mode for 3 secs. Then the motor is made to run in

forward mode at 150 rad/sec upto t=6.5 sec. The motor is then made to run in reverse motoring mode at -150 rad/sec upto t=10.5 sec. The motor is then made to run at -100 rad/sec upto t=14 sec and then finally made to run at 100rad/sec.

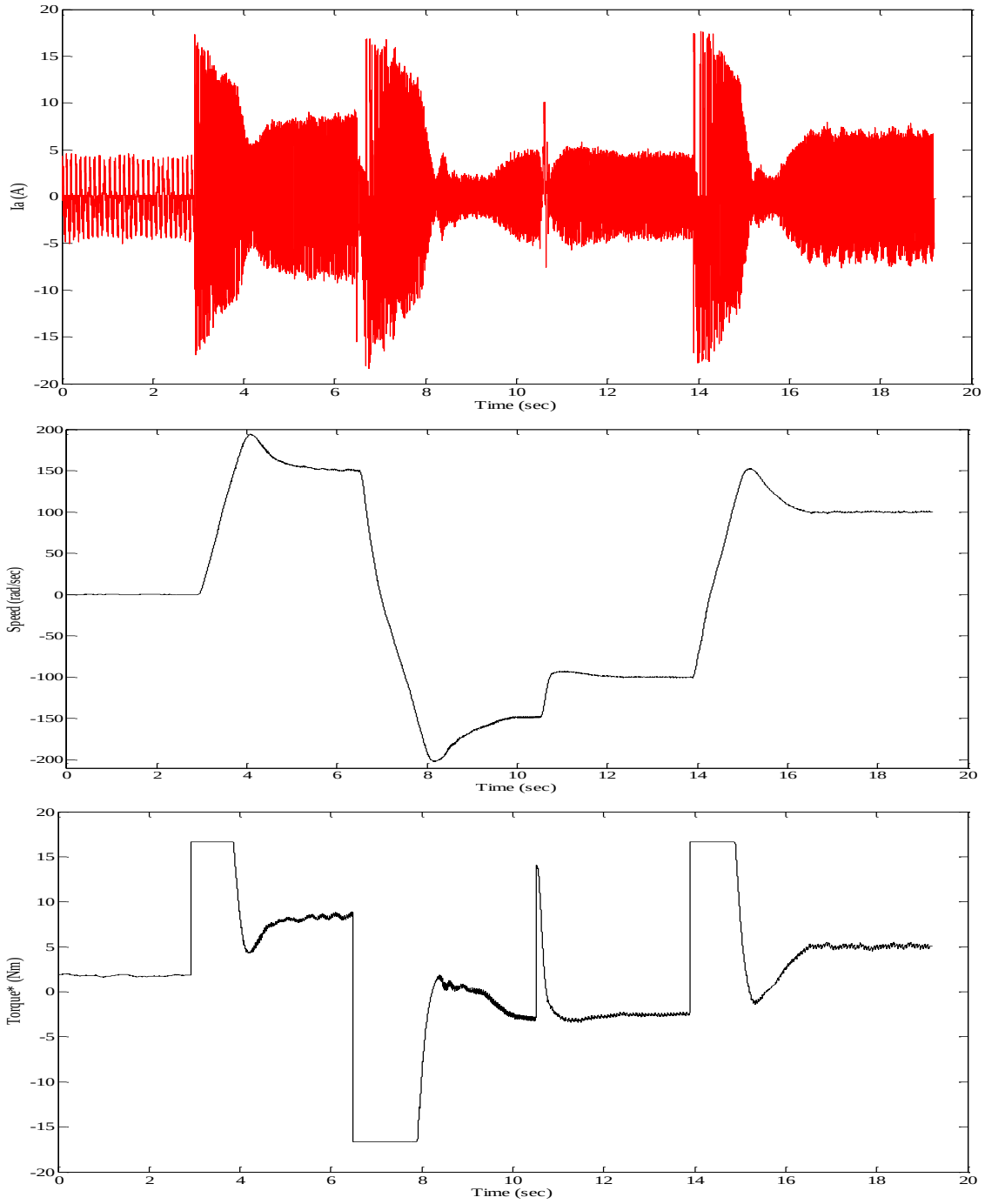

Fig. 4.6 Experimental Performance of IVCIM using PI controller in forward, reverse and braking mode

The performance of IVCIM is also dependent on the Hysteresis current controller. A change in Hysteresis band changes the switching frequency of the IGBT. A higher value of Hysteresis band is tried out experimentally using a PI controller and the performance of the IVCIM is shown in Fig. 4.7. It is observed that speed and current take longer time to reach steady state. Also the pulsations in torque have increased meaning poorer operation.

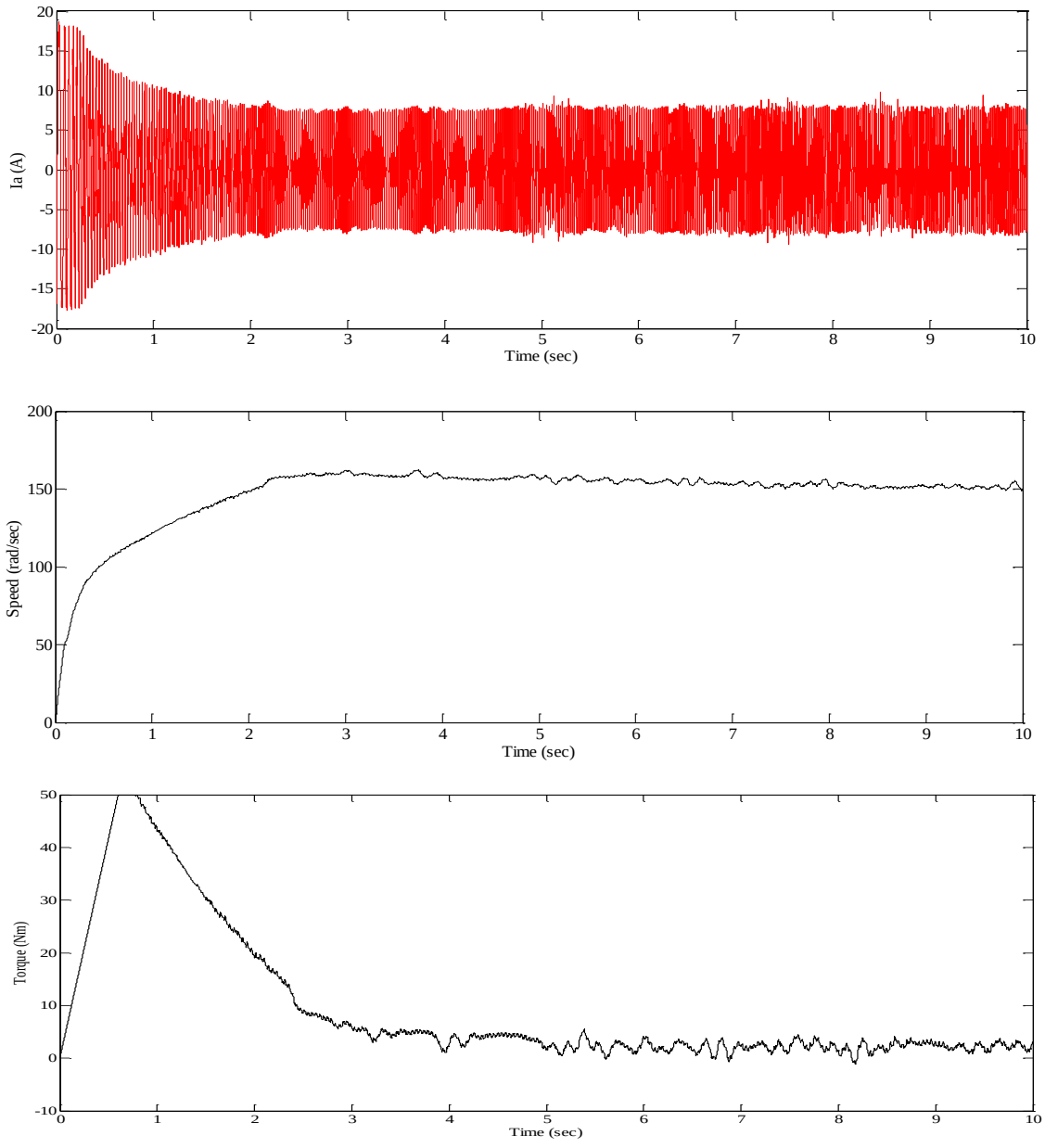

Fig. 4.7 Experimental Performance of IVCIM using PI controller with Hysteresis Band=5 in current controller

4.5.2 Performance of IVCIM using Fuzzy Logic Controller

The dynamic operation of IVCIM is also studied using FLC speed controller. The real time behavior under no-load and load conditions is studied.

Fig. 4.8 shows the performance of IVCIM using Fuzzy logic controller as obtained experimentally. The figure shows the line current (i_a), the speed (ω) and the electromagnetic torque (T_e) developed by the motor.

Initially no load is applied to the Induction motor. The starting characteristics of the motor show high starting current. The motor is set to a rated speed of 150 rad/sec. The performance of FLC as observed shows its superior performance over PI controller as the motor takes just 2 sec to reach rated speed. The starting current is high, but eventually the steady state current of 5 A is reached at no load in 1.2 sec.

At t=4.2 sec, a load torque of 7 Nm is applied at the motor shaft, which increases the motor current to 7.5 A and also there is a momentary dip in the motor speed. However the Fuzzy Logic controller regulates the speed of motor to 150 rad/sec within 0.3 sec.

Comparing the results as obtained from FLC based IVCIM and from PI based IVCIM; experimentally show that the FLC has superior performance over the PI controller. The FLC based IVCIM drive shows better speed and torque control. The speed control is more efficient and also the torque pulsations are less.

From Fig. 4.3 and Fig. 4.8, it is observed that the Fuzzy Logic controller regulates the speed transition from zero to rated speed more smoothly and quickly, through simulation in MATLAB as well as experimentally. Also on application of load, there is a momentary dip in speed, but Fuzzy Logic controller is able to recover the speed much more quickly than compared to the PI controller.

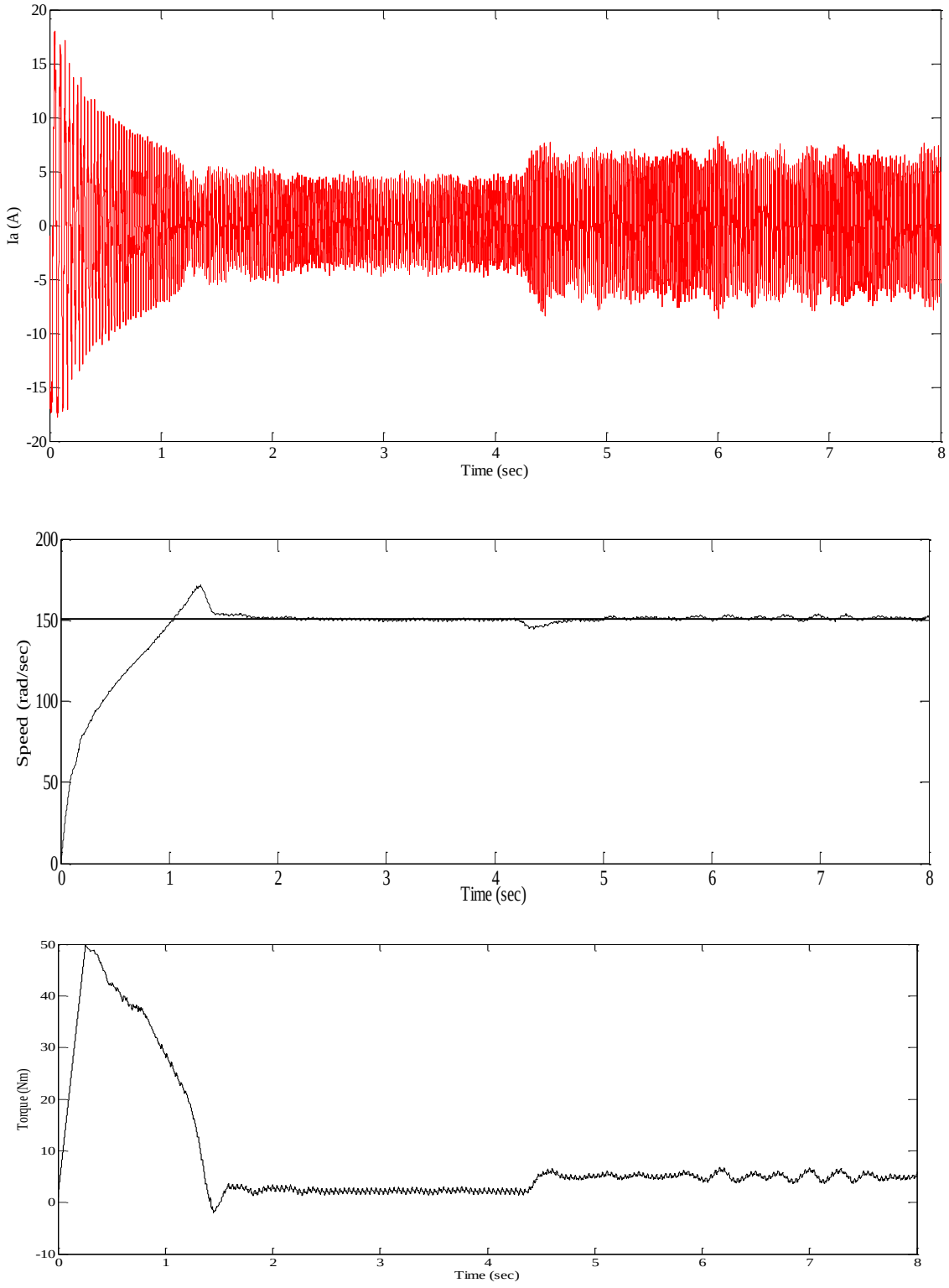

Fig. 4.8 Experimental Performance of IVCIM using Fuzzy logic controller

Fig. 4.9 shows steady state value of line currents (i_a, i_b, i_c) at (a) no load (b) load. The performance of FLC in regulating current can be observed. Comparing these results with that of Fig. 4.5, it is observed that the FLC regulates the current in a better fashion as compared to PI controller. The current profile shows more harmonics at no load compared to the load current. The harmonics in case of FLC based controller have been reduced compared to that of PI based IVCIM.

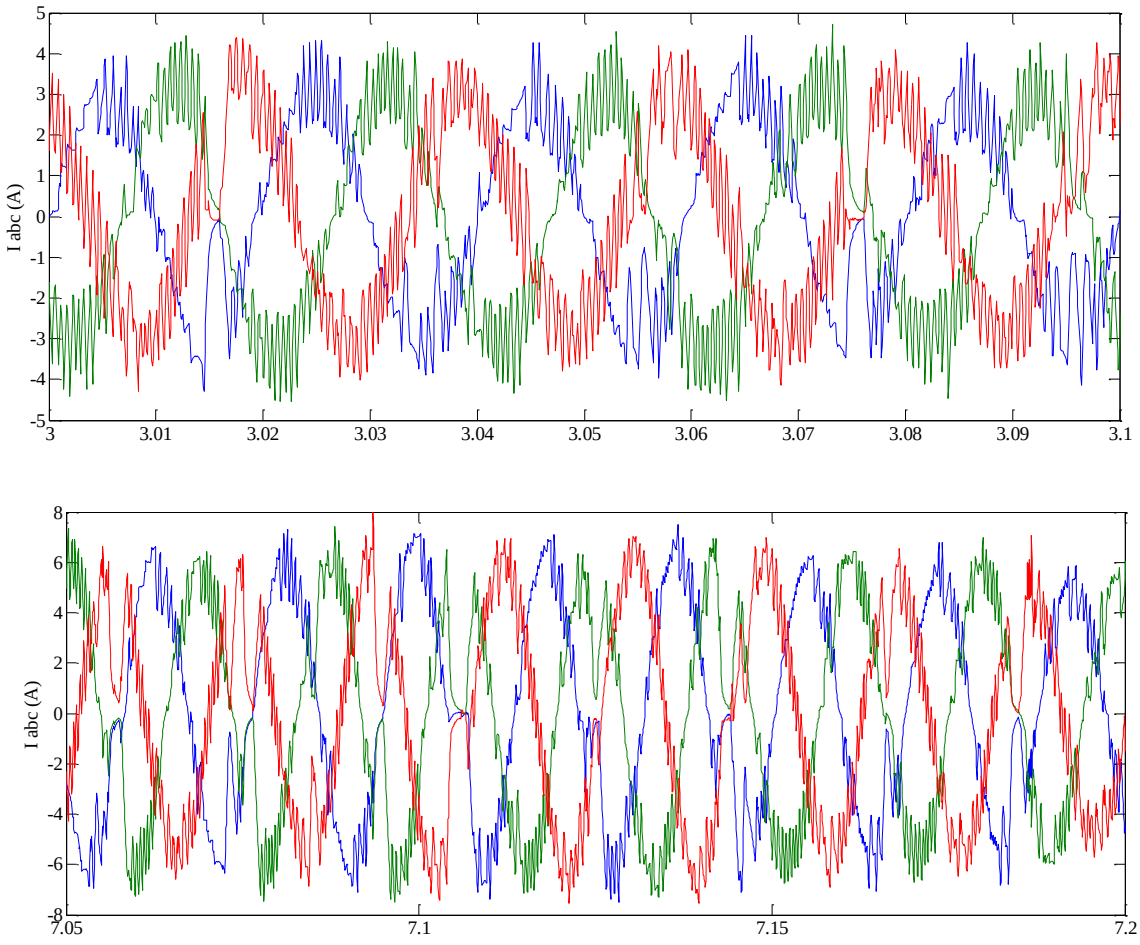

Fig. 4.9 Steady state value of line currents (i_a, i_b, i_c) at (a) no load (b) load

Again the performance of FLC in regulating the motor in forward, reverse motoring mode and braking mode is studied and shown in Fig. 4.10. The figure shows the line current (i_a), the speed (ω) and the electromagnetic torque (T_e) developed by the motor. Initially the motor shaft is plugged for 2 secs. The motor speed is set to 150 rad/sec in forward motoring mode. Then the motor is set in reverse motoring mode at -50 rad/sec at

t=5.5sec. Then the motor is set at -150 rad/sec at t=8.5 sec. The motor speed is changed to 50 rad/sec at t=12.5 sec. The motor is then again set to 150 rad/sec at t=16.5 sec. The speed regulation of motor in all the three modes is significantly improved with FLC. The overshoots in speed are reduced with FLC.

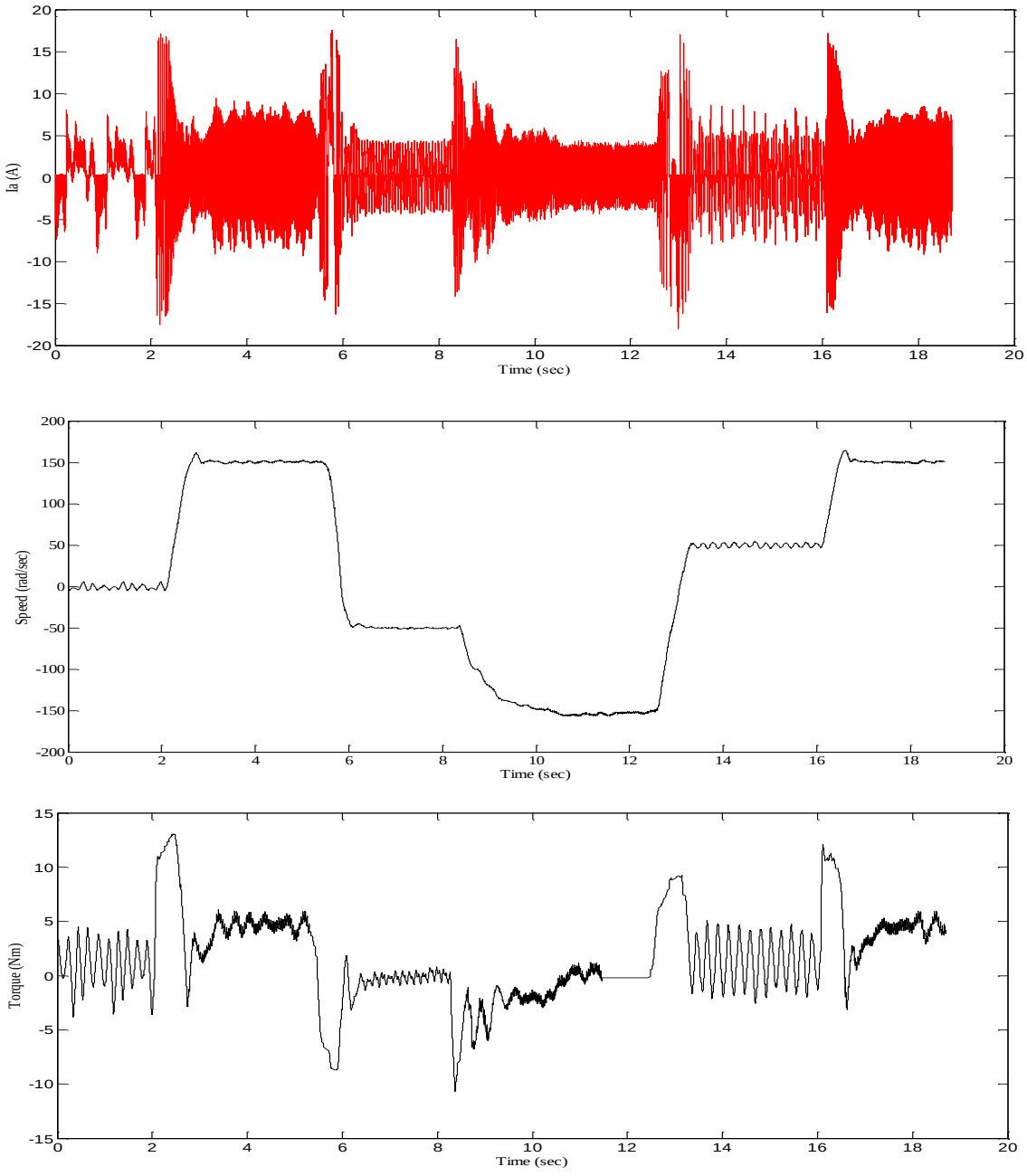

Fig. 4.10 Experimental Performance of IVCIM using FLC in forward, reverse and braking mode

Similar to PI controller, a higher value of Hysteresis band is tried out experimentally using an FLC and the performance of the IVCIM is shown in Fig. 4.11. Again it is observed that speed and current take longer time to reach steady state. It is observed that the effect of change in hysteresis band is more prominent in FLC.

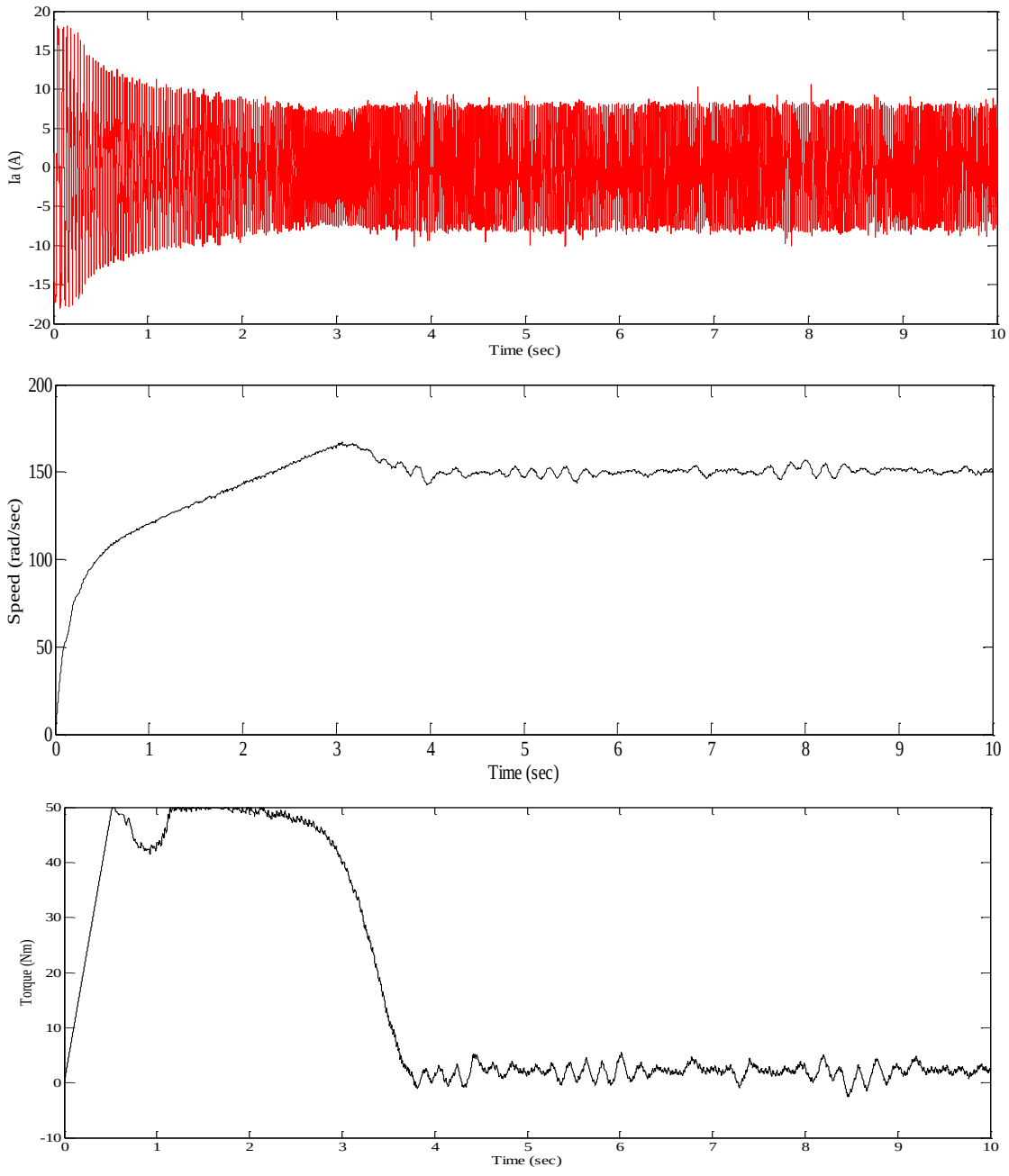

Fig. 4.11 Experimental Performance of IVCIM using FLC with Hysteresis Band=5 in current controller

4.6 Comparison of performance of PI and FLC speed controller

Fig. 4.12 shows the comparison of the performance of the two controllers in attaining the desired speed through simulation in MATLAB/Simulink. The speed in case of FLC sets to 150 rad/sec even before the application of the load, which is not the case with PI controller. The settling time for FLC scheme is 0.037 sec. After application of load, FLC regains the value in 0.05 sec whereas PI controller regains the value in 0.1 sec.

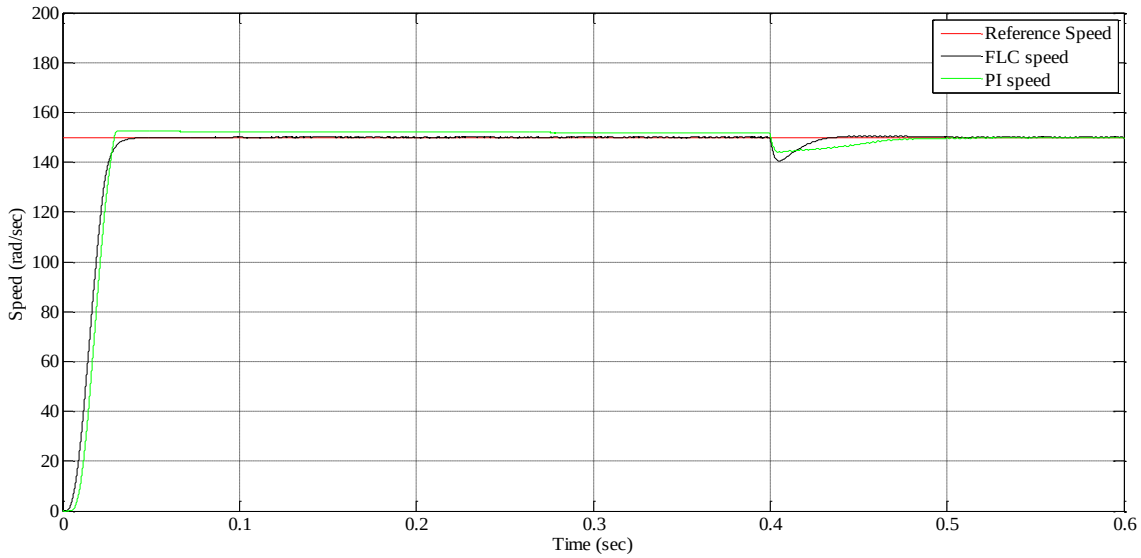

Fig. 4.12 Comparison of Speed deviation in PI & Fuzzy Logic Controllers

4.7 Conclusion

The results obtained from simulation in MATLAB and experimentally show superior performance of the drive with FLC. The FLC results in quicker transition from zero to rated speed. Also on application of load, the FLC shows quicker response to reach steady state as compared to PI controller. The current profile is better in case of FLC. The performance of FLC in forward, reverse and braking mode is also better than PI controller.

Chapter V

Conclusion and Future Scope

5.1 Main Conclusions

In this project, an extensive review of PI and FLC controllers and feedback signal estimation techniques for squirrel cage-type induction motor drives is carried out. This class of drives is widely gaining popularity in various industrial applications, and the technology is continuously expanding. An intimate understanding of machine performance, under different operating conditions, is necessary to design modern high-performance drives. Often, for a particular application, where more than one type of machines is being used, this analysis is necessary.

Vector control was discussed extensively because of its importance in high-performance drive applications. The vector control implementation with corresponding feedback signal estimation is complex. The Fuzzy Logic Controller was reviewed in this thesis. The results are obtained in both MATLAB/Simulink and in real time through hardware implementation.

The comparison between the two techniques shows that the FLC has a robust performance. The transient response is smoother in case of FLC. Also during sudden load changes, the response obtained from the Fuzzy Logic Controller is better. The FLC eliminates the transients during sudden change in load as compared to that of PI controller. On the other hand the PI controller shows significant variations to change in load conditions. The response of FLC is faster than PI controller. The characteristics of the drives are obtained and verified for the forward and reverse motoring mode and as well for plugging mode.

The results from both simulation in MATLAB/Simulink and hardware confirm the conclusion.

5.2 Future Scope of the Work

A number of control techniques are available that can be implemented to improve the performance of the AC drives.

The conventional PID technique implementation in real time requires tuning of three parameters which is not simple and easy to achieve in real time. The implementation of the PI controller is relatively simple but the performance of the drive deteriorates due to variations in motor parameters. The PI & FLC can be implemented in hybrid mode to obtain a better performance.

The FLC scheme used in this project is a Type I FLC. A Type II FLC can also be implemented to improve the performance in non-linear region. The Neural Network techniques are being studied presently. The recent trend of the utilization of ANFIS, which is a hybrid of Fuzzy and Neural Network control algorithms, has also shown, wide potential for application in high performance IM drives.

Besides this, in the present analysis, the hysteresis current control technique has been used for control of VSI, however, the SVPWM technique reduces the computational time of the processors. A synchronous current control voltage PWM can also be used.

Speed Sensorless vector control is an emerging technology. A number of speed estimation techniques are being reviewed. However, very low-speed operation including start-up at zero frequency remains a challenge.

Besides Sensorless Vector Control Scheme, there is also Direct Torque Control Scheme. Its response has been found to be more superior to FOC scheme. Torque and flux are changed very fast by changing the references. High efficiency and low losses - switching losses are minimized because the transistors are switched only when it is needed to keep torque and flux within their hysteresis bands.

Appendix A

Rating and parameters of three-phase Induction Motor

The induction motor used in the MATLAB simulation & the hardware has the following specifications:

3-phase Squirrel cage induction motor, Δ- Connected,

Power rating, 3hp (2.238KW)

Stator rms voltage, 230 V (50 Hz)

Rated stator Current, 8.5 A

Rated Speed, 1440rpm (150 rad/sec)

Rs, stator resistance, 3.3 Ω

Rr, rotor resistance, 3.22 Ω

Ls, stator inductance, 0.0133 H

Lr, rotor inductance, 0.0133 H

Lm, magnetizing inductance, 0.144 H

J, moment of inertia, 0.002 Kg m^2

P, number of poles, 4

Appendix B

Hysteresis Current Controller

In this circuit three phase load is connected to the PWM voltage source inverter. The load currents *ia, ib* and *ic* are compared with the reference currents *ia*, ib** and *ic** and error signals are passed through hysteresis band to generate the firing pulses, which are operated to produce output voltage in manner to reduce the current error.

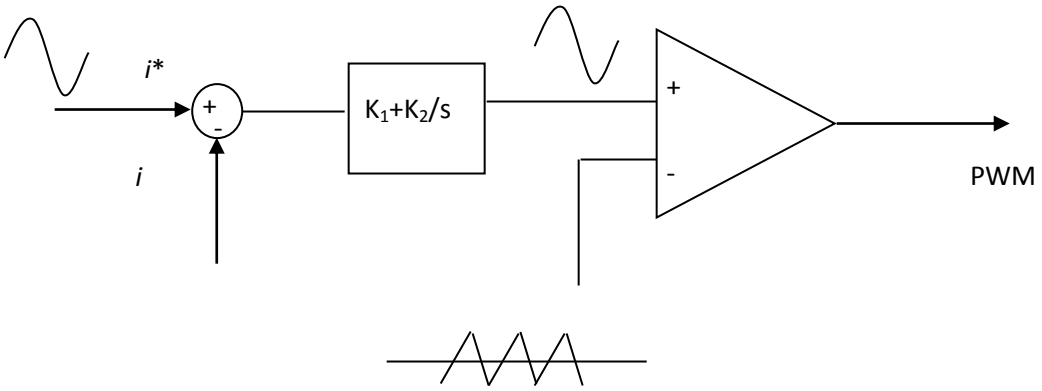

Fig. PWM obtained from hysteresis current control

The principle of Hysteresis current control is very simple. The purpose of the current controller is to control the load current by forcing it to follow a reference one. It is achieved by the switching action of the inverter to keep the current within the Hysteresis band. The load currents are sensed & compared with respective command currents by three independent Hysteresis comparators having a hysteresis band '*h*'. The output signals of the comparators are used to activate the inverter power switches. The inverter current vector is defined as

$$\boldsymbol{i} = \frac{\mathbf{2}}{\mathbf{3}}[\boldsymbol{i_a} + \boldsymbol{a i_b} + \boldsymbol{a^2 i_c}]$$

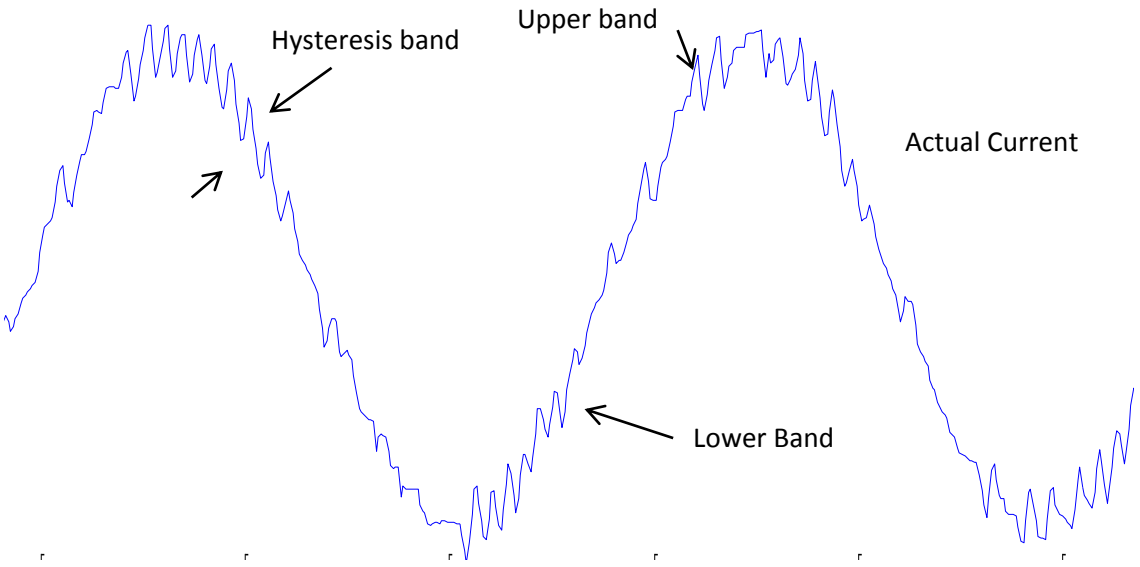

Fig. An actual current waveform obtained from Hysteresis Current Control

In this scheme, the hysteresis bands are fixed throughout the fundamental period. The algorithm for this scheme is given as

$$\boldsymbol{Iref} = \boldsymbol{I\,maxsin\omega t}$$

Upper band

$$\boldsymbol{iup} = \boldsymbol{iref} + \boldsymbol{h}$$

Lower band

$$\boldsymbol{ilow} = \boldsymbol{iref} - \boldsymbol{h}$$

Where *h* = Hysteresis band limit

$$\text{If } \boldsymbol{ia} > \boldsymbol{iup},\ \boldsymbol{Vao} = -\boldsymbol{Vdc/2}$$
$$\text{If } \boldsymbol{ia} < \boldsymbol{ilow},\ \boldsymbol{Vao} = +\boldsymbol{Vdc/2}$$

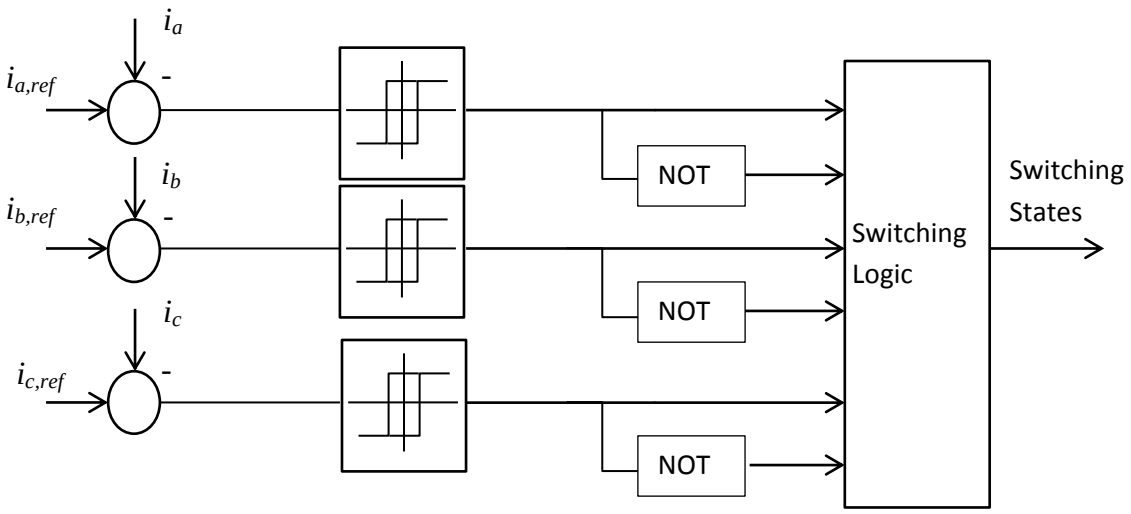

Fig. Structure of Hysteresis Current Controller

Appendix C

ABB Voltage Sensor

EM010-9237

U_{PN} = 200V

V_A = ±12 V…24 V

R_E = 10 K

R_M = 4.7 K

ABB voltage sensors based on closed loop Hall Effect technology are also electronic transformers. They allow for the measurement of direct, alternating and impulse voltages with galvanic insulation between the primary and secondary circuits. The primary voltage UP to be measured is applied directly to the sensor terminals: HT+ (positive high voltage) and HT– (negative high voltage).

An input resistance R_E must necessarily be placed in series with the resistance R_P of the primary winding to limit the current I_P and therefore the heat dissipated from the sensor. This resistance R_E may be either integrated during the manufacturing of the product (calibrated sensor) or added externally by the user to determine the voltage rating (not calibrated sensor).

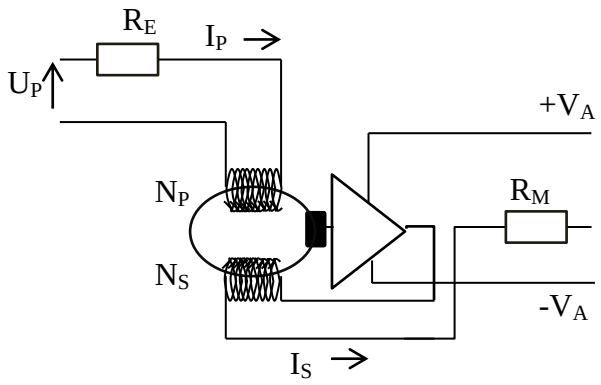

Fig. Principal diagram of EM010 Sensor

The primary current I_P flowing across the primary winding via this resistance R_E generates a primary magnetic flux. The magnetic circuit channels this magnetic flux. The Hall probe placed in the air gap of the magnetic circuit provides a voltage V_H proportional to this flux.

The electronic circuit amplifies this voltage and converts it into a secondary current I_S. This secondary current multiplied by the number of turns N_S of secondary winding cancels out the primary magnetic flux that created it (contra reaction).
The formula

$$N_P * I_P = N_S * I_S$$

is true at any time. The voltage sensor measures instantaneous values. The secondary output current 'I_S' is therefore exactly proportional to the primary voltage at any moment. It is an exact replica of the primary voltage. This secondary current 'I_S' is passed through a measuring resistance R_M. The measuring voltage V_M at the terminals of this measuring resistance R_M is therefore also exactly proportional to the primary voltage U_P.

ABB Current Sensor

EH050AP

I_{PN} = 50 A

V_A = ±12 V…24 V

R_E = 10 K

R_M = 330 Ω

ABB current sensors based on closed loop Hall Effect technology are electronic transformers. They allow for the measurement of direct, alternating and impulse currents, with galvanic insulation between the primary and secondary circuits. The primary current I_P flowing across the sensor creates a primary magnetic flux. The magnetic circuit channels this magnetic flux. The Hall probe placed in the air gap of the magnetic circuit provides a voltage proportional to this flux. The electronic circuit amplifies this voltage and converts it into a secondary current I_S. This secondary current multiplied by the number of turns N_S of secondary winding cancels out the primary magnetic flux that created it (contra reaction). The formula

$$N_P * I_P = N_S * I_S$$

is true at any time. The current sensor measures instantaneous values.

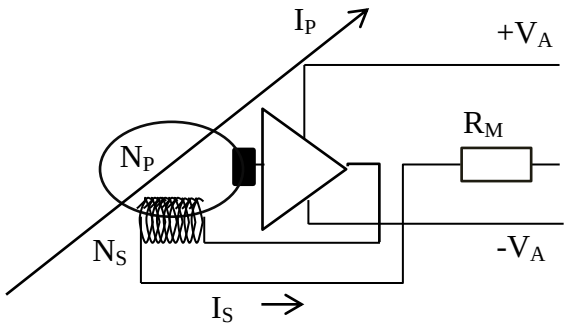

Fig. Principal Diagram of ABB Current Sensor

The secondary output current 'I_S' is therefore exactly proportional to the primary current at any moment. It is an exact replica of the primary current multiplied by the number of turns N_P/N_S. This secondary current I_S can be passed through a measuring resistance R_M. The measuring voltage V_M at the terminals of this measuring resistance R_M is therefore also exactly proportional to the primary current I_P.

Appendix D

DS-1104 technical specifications

Main Processor:	• MPC8240, PowerPC 603e core, 250 MHz • 32 kByte internal cache
Timers:	• 1 sample rate timer, 32-bit downcounter • 4 general purpose timers, 32 bit • 64-bit timebase for time measurement
Memory:	• 32 MByte synchronous DRAM (SDRAM) • 8 MByte boot flash for applications
Interrupt Control Unit:	• Interrupts by timers, serial interface, slave DSP, incremental encoders, ADC, host PC and 4 external inputs • PWM synchronous interrupts
Analog Input:	• 4 ADC inputs, 16 bit, multiplexed • ± 10 V input voltage range • 2µs sampling time • >80 dB signal-to-noise ratio • ADC channels, 12 bit • ± 10 V input voltage range • 800 ns sampling time • > 65 dB signal-to-noise ratio
Analog Output:	• 8 channels, 16 bit, 10 µs max. settling time • ± 10 V output voltage range
Incremental Encoder: **Interface:**	• Two digital inputs, TTL or RS422 • 24-bit digital incremental encoders • Max. 1.65 MHz input frequency, i.e. fourfold pulse counts up to 6.6 MHz • 5 V / 0.5 A sensor supply voltage

Digital I/O:	• 20-bit digital I/O (bit-selectable direction) • ± 5 mA output current
Serial Interface:	• Serial UART (RS232, RS485 and RS422)
Slave DSP Subsystem:	• Texas Instruments' DSP TMS320F240 • 4 kWord of dual-port RAM • Three-phase PWM outputs plus 4 single PWM outputs • 14 bits of digital I/O (TTL)
Physical Characteristics:	• Power supply 5 V, 2.5 A / -12 V, 0.2 A /12 V, 0.3 A • Requires one 32-bit PCI slot

REFERENCES

1. F. Blaschke, "Das Verfahren Der Feldorientierung Zur Regelung Der Asynchronmaschine", *Siemens Forschungs-und Entwicklungsberichte 1, 1972.*
2. K. Hasse, '"Zur dynamik drehzahlgeregelter antriebe mit stromrichtergespeisten asynchrony-kurzschlublaufenn- aschinen", *Darmstadt, Techn. Hochsch., Diss., 1969.*
3. Rupprecht Gabriel. Werner Leonhard, and Craig J. Nordby, "Field-Oriented Control of a Standard AC Motor Using Microprocessors", *IEEE Transactions On Industrial Applications Vol. IA-16, No. 2, March/April 1980*
4. Takayoshi Matsuo and Thomas A. Lipo, "A Rotor Parameter Identification Scheme forVector-Controlled Induction Motor Drives", *IEEE Transactions On Industry Applications, Vol. IA-21, No. 4, May/June 1985*
5. David M. Brod, and Donald W. Novotny, "Current Control of VSI-PWM Inverters", *IEEE Transactions On Industry Applications, Vol. IA-21. No. 4, May/June 1985*
6. Masato Koyama, Masao Yano, Isao Kamiyama, And Sadanari Yano, "Microprocessor-Based Vector Control System For Induction Motor Drives With Rotor Time Constant Identification Function", *IEEE Transactions on Industry Applications, Vol. Ia-22, No. 3, May/June 1986*
7. Isao Takahashi, and Toshihiko Noguchi, "A New Quick-Response and High-Efficiency Control Strategy of an Induction Motor", *IEEE Transactions on Industry Applications, Vol. Ia-22, No. 5. September/October 1986*
8. Isao Takahashi, Member IEEE, Youichi Ohmori, "High-Performance Direct Torque Control Of An Induction Motor, IEEE Transactions On Industry Applications", *Vol. 25, No. 2, March/April 1989*
9. Toshiaki Murata, Takeshi Tsuchiya, I Kuo Takeda, "Vector Control For Induction Machine On The Application Of Optimal Control Theory", *IEEE Transactions On Industrial Electronics, Vol. 31, No. 4, August 1990*

10. Marian P. Kazmierkowski And Waldemar Sulkowski, “A Novel Vector Control Scheme For Transistor PWM Inverter-Fed Induction Motor Drive”, *IEEE Transactions On Industrial Electronics, Vol. 38, No. 1, February 1991*
11. Ramu Krishnan, and Aravind S. Bharadwaj, “A Review Of Parameter Sensitivity And Adaptation In Indirect Vector Controlled Induction Motor Drive Systems”, *IEEE Transactions On Power Electronics Vol 6 No -1 October 1991*
12. Tsugutoshi Ohtani, Noriyuki Takada, And Koji Tanaka, “Vector Control Of Induction Motor Without Shaft Encoder”, *IEEE Transactions On Industry Applications, Vol. 28, No. 1, January/February 1992*
13. Yau-Tze Kao And Chang-Huan Liu”, “Analysis And Design Of Microprocessor-Based Vector-Controlled Induction Motor Drives”, *IEEE Transactions On Industrial Electronics, Vol. 39, No.1, February 1992*
14. Colin Schauder, “Adaptive Speed Identification For Vector Control Of Induction Motors Without Rotational Transducers”, *IEEE Transactions On Industry Applications, Vol. 28, No. 5, September/October 1992*
15. Ching-Tsai Pan, Ting-Yu Chang, “A Microcomputer Based Vector Controlled Induction Motor Drive”, *IEEE Transactions On Energy Conversion, Vol. 8, No. 4, December 1993*
16. Ting-Yu Chang And Ching-Tsai Pan, “A Practical Vector Control Algorithm For P-Based Induction Motor Drives Using A New Space Vector Current Controller”, *IEEE Transactions On Industrial Electronics. Vol.41, No.1, February 1994*
17. Ting-Yu Chang, Kuie-Lin Lo, and Ching-Tsai Pan, “A Novel Vector Control Hysteresis Current Controller For Induction Motor Drives”, *IEEE Transactions On Energy Conversion, Vol. 9, No. 2, June 1994*
18. Kanokvate Tungpimolrut, Fang-Zheng Peng, and Tadashi Fukao, “Robust Vector Control Of Induction Motor Without Using Stator And Rotor Circuit Time Constants”, *IEEE Transactions On Industry Applications, Vol. 30, No. 5, September / October 1994*
19. Fang-Zheng Peng, and Tadashi Fukao, “Robust Speed Identification For Speed-Sensorless Vector Control Of Induction Motors”, *IEEE Transactions On Industry Applications, Vol. 30, No.5, September / October 1994*

20. Gilbert0 C. D. Sousa, Bimal K. Bose, and John G. Cleland, “Fuzzy Logic Based On-Line Efficiency Optimization Control Of An Indirect Vector-Controlled Induction Motor Drive”, *IEEE Transactions On Industrial Electronics, Vol. 42, No. 2, April 1995*
21. M. Godoy Simces, and Bimal K. Bose, “Neural Network Based Estimation Of Feedback Signals For A Vector Controlled Induction Motor Drive”, *IEEE Transactions On Industry Applications, Vol. 31, No. 3, May/June 1995*
22. Marian P. Kazmierkowski, and Andrzej B. Kasprowicz, “Improved Direct Torque And Flux Vector Control Of PWM Inverter-Fed Induction Motor Drives”, *IEEE Transactions On Industrial Electronics, Vol. 42. No. 4, August 1995*
23. S.Williamson, R.C. Healey, “Space Vector Representation Of Advanced Motor Models For Vector Controlled Induction Motors”, *IEE Proc-Electr, Power Appl., Vol. 143, No. I, January 1996*
24. A.Hughes, J.Corda, D.A.Andrade, “Vector Control Of Cage Induction Motors: A Physical Insight”, *IEE Proc-Electr, Power Appl., Vol. 143, No.1, January 1996*
25. Susumu Tadakuma, Shigeru Tanaka, Haruo Naitoh, and Kazuo Shimane**,** **“**Improvement Of Robustness Of Vector-Controlled Induction Motors Using Feedforward And Feedback Control”, *IEEE Transactions On Power Electronics, Vol. 12, No. 2, March 1997*
26. Bimal K. Bose, Nitin R. Patel, and Kaushik Rajashekara “A Neuro–Fuzzy-Based On-Line Efficiency Optimization Control of a Stator Flux-Oriented Direct Vector-Controlled Induction Motor Drive”, *IEEE Transactions On Industrial Electronics, Vol. 44, No. 2, April 1997*
27. James N. Nash, “Direct Torque Control, Induction Motor Vector Control without An Encoder”, *IEEE Transactions On Industry Applications, Vol. 33, No. 2, March/April 1997*
28. Bimal K. Bose, Nitin R. Patel, And Kaushik Rajashekara, “A Start-Up Method For A Speed Sensorless Stator-Flux- Oriented Vector-Controlled Induction Motor Drive”, *IEEE Transactions on Industrial Electronics, Vol. 44, No. 4, August 1997*

29. Emanuele Cerruto, Alfio Consoli, Angelo Raciti, and Antonio Testa, "Fuzzy Adaptive Vector Control Of Induction Motor Drives", *IEEE Transactions On Power Electronics, Vol. 12, No. 6, November 1997*
30. Yi-Hwa Liu, Chern-Lin Chen, and Rong-Jie Tu, "A Novel Space-Vector Current Regulation Scheme For A Field-Oriented-Controlled Induction Motor Drive", *IEEE Transactions On Industrial Electronics, Vol. 45, No. 5, October 1998*
31. Y.S. Lai, S.C.Chang, "DSP-Based Implementation of New Random Switching Technique Of Inverter Control For Sensorless Vector-Controlled Induction Motor Drives", *IEE Proc.-Electr. Power Appl., Vol. 146, No. 2, March 1999*
32. Yoshitaka Kawabata, Emenike Ejiogu, and Takao Kawabata, "Vector-Controlled Double-Inverter-Fed Wound-Rotor Induction Motor Suitable For High-Power Drives", *IEEE Transactions On Industry Applications, Vol. 35, No. 5, September/October 1999*
33. Y. S. Lai, "Sensorless Speed Vector-Controlled Induction Motor Drives Using New Random Technique for Inverter Control", *IEEE Transactions On Energy Conversion, Vol. 14, No. 4, December 1999*
34. J.W.L.Nerys, A.Hughes and J.Corda, "Alternative Implementation Of Vector Control For Induction Motor And Its Experimental Evaluation", *IEE Proc-Eleclr, Power Appl., Vol. 147, No. 1, January 2000*
35. Yen-Shin Lai, and Ye-Then Chang, "Design And Implementation Of Vector-Controlled Induction Motor Drives Using Random Switching Technique With Constant Sampling Frequency", *IEEE Transactions On Power Electronics, Vol. 16, No. 3, May 2001*
36. João O. P. Pinto, Bimal K. Bose, and Luiz Eduardo Borges Da Silva, "A Stator-Flux-Oriented Vector-Controlled Induction Motor Drive With Space-Vector PWM And Flux-Vector Synthesis By Neural Networks", *IEEE Transactions On Industry Applications, Vol. 37, No. 5, September/October 2001*
37. Epaminondas D. Mitronikas, Athanasios N. Safacas, and Emmanuel C. Tatakis, "A New Stator Resistance Tuning Method For Stator-Flux-Oriented Vector-Controlled Induction Motor Drive", *IEEE Transactions On Industrial Electronics, Vol. 48, No. 6, December 2001*

38. F. Barrero, A. González, A. Torralba, E. Galván, And L. G. Franquelo, "Speed Control Of Induction Motors Using A Novel Fuzzy Sliding-Mode Structure", *IEEE Transactions On Fuzzy Systems, Vol. 10, No. 3, June 2002*
39. Joachim Holtz, and Juntao Quan, "Sensorless Vector Control Of Induction Motors At Very Low Speed Using A Nonlinear Inverter Model And Parameter Identification", *IEEE Transactions On Industry Applications, Vol. 38, No. 4, July/August 2002*
40. M. Nasir Uddin, Tawfik S. Radwan, and M. Azizur Rahman, "Performances Of Fuzzy-Logic-Based Indirect Vector Control For Induction Motor Drive", *IEEE Transactions On Industry Applications, Vol. 38, No. 5, September/October 2002*
41. Kouki Matsuse, Yuusuke Kouno, Hirotoshi Kawai, And Shinichi Yokomizo, "A Speed-Sensorless Vector Control Method Of Parallel-Connected Dual Induction Motor Fed By A Single Inverter", *IEEE Transactions On Industry Applications, Vol. 38, No. 6, November/December 2002*
42. Chandan Chakraborty, and Yoichi Hori, "Fast Efficiency Optimization Techniques For The Indirect Vector-Controlled Induction Motor Drives", *IEEE Transactions On Industry Applications, Vol. 39, No. 4, July/August 2003*
43. E. Levi, M. Jones And S.N. Vukosavic, "Even-Phase Multi-Motor Vector Controlled Drive With Single Inverter Supply And Series Connection Of Stator Windings", *IEE Proc.-Electr. Power Appl., Vol. 150, No. 5, September 2003*
44. Masaru Hasegawa, Shinichi Furutani, Shinji Doki, and Shigeru Okuma, "Robust Vector Control Of Induction Motors Using Full-Order Observer In Consideration Of Core Loss", *IEEE Transactions On Industrial Electronics, Vol. 50, No. 5, October 2003*
45. Yoshitaka Kawabata, Tomoyuki Kawakami, Yoshiki Sasakura, Emenike C. Ejiogu, and Takao Kawabata, "New Design Method Of Decoupling Control System For Vector Controlled Induction Motor", *IEEE Transactions On Power Electronics, Vol. 19, No. 1, January 2004*
46. Maurício Beltrão De Rossiter Corrêa, Cursino Brandão Jacobina, Edison Roberto Cabral Da Silva, and Antonio Marcus Nogueira Lima, "Vector Control Strategies

For Single-Phase Induction Motor Drive Systems", *IEEE Transactions On Industrial Electronics, Vol. 51, No. 5, October 2004*

47. Maria Imecs, Andrzej M. Trzynadlowski, Ioan I. Incze, And Csaba Szabo, "Vector Control Schemes For Tandem-Converter Fed Induction Motor Drives", *IEEE Transactions On Power Electronics, Vol. 20, No. 2, March 2005*
48. Mika Salo And Heikki Tuusa, "A Vector-Controlled PWM Current-Source-Inverter-Fed Induction Motor Drive With A New Stator Current Control Method", *IEEE Transactions On Industrial Electronics, Vol. 52, No. 2, April 2005*
49. G. K. Singh, K. Nam, and S. K. Lim, "A Simple Indirect Field-Oriented Control Scheme For Multiphase Induction Machine", *IEEE Transactions On Industrial Electronics, Vol. 52, No. 4, August 2005*
50. Epaminondas D. Mitronikas And Athanasios N. Safacas, "An Improved Sensorless Vector-Control Method For An Induction Motor Drive", *IEEE Transactions On Industrial Electronics, Vol. 52, No. 6, December 2005*
51. Mihai Comanescu, and Longya Xu, "An Improved Flux Observer Based On PLL Frequency Estimator For Sensorless Vector Control Of Induction Motors", *IEEE Transactions On Industrial Electronics, Vol. 53, No. 1, February 2006*
52. Bhim Singh, G. Bhuvaneswari, And Vipin Garg, "Power-Quality Improvements In Vector-Controlled Induction Motor Drive Employing Pulse Multiplication In Ac–Dc Converters", *IEEE Transactions On Power Delivery, Vol. 21, No. 3, July 2006*
53. Radu Bojoi, Alberto Tenconi, Giovanni Griva, and Francesco Profumo, "Vector Control Of Dual-Three-Phase Induction-Motor Drives Using Two Current Sensors", *IEEE Transactions On Industry Applications, Vol. 42, No. 5, September/October 2006*
54. S. Drid, M. Tadjine and M.S. Nai¨T-Sai¨D, "Robust Backstepping Vector Control For The Doubly Fed Induction Motor", *IET Control Theory Appl., 2007, 1, (4), Pp. 861–868*
55. Bhim Singh, Vipin Garg, and G. Bhuvaneswari, "Polygon-Connected Autotransformer-Based 24-Pulse Ac–Dc Converter For Vector-Controlled

Induction-Motor Drives", *IEEE Transactions On Industrial Electronics, Vol. 55, No. 1, January 2008*

56. Michele Mengoni, Luca Zarri, Angelo Tani, Giovanni Serra, and Domenico Casadei, "Stator Flux Vector Control Of Induction Motor Drive In The Field Weakening Region", *IEEE Transactions On Power Electronics, Vol. 23, No. 2, March 2008*
57. Bhim Singh, and Sanjay Gairola, "A 40-Pulse Ac–Dc Converter Fed Vector-Controlled Induction Motor Drive", *IEEE Transactions On Energy Conversion, Vol. 23, No. 2, June 2008*
58. R. Gregor, F. Barrero, S.L. Toral, M.J. Dura´N, M.R. Arahal, J. Prieto, J.L. Mora, "Predictive-Space Vector PWM Current Control Method For Asymmetrical Dual Three-Phase Induction Motor Drives", *Published In IET Electric Power Applications, Received On 24th November 2008, Revised On 14th April 2009, Doi: 10.1049/Iet-Epa.2008.0274*
59. Andrew Trentin, Pericle Zanchetta, Chris Gerada, Jon Clare, and Patrick W. Wheeler, "Optimized Commissioning Method For Enhanced Vector Control Of High-Power Induction Motor Drives", *IEEE Transactions On Industrial Electronics, Vol. 56, No. 5, May 2009*
60. Young-Su Kwon, Jeong-Hum Lee, Sang-Ho Moon, Byung-Ki Kwon, Chang-Ho Choi, and Jul-Ki Seok, "Standstill Parameter Identification Of Vector-Controlled Induction Motors Using The Frequency Characteristics Of Rotor Bars", *IEEE Transactions On Industry Applications, Vol. 45, No. 5, September/October 2009*
61. David C. Meeker, and Michael John Newman, "Indirect Vector Control Of A Redundant Linear Induction Motor For Aircraft Launch", *IEEE | Vol. 97, No. 11, November 2009*
62. M.E. Romero, M.M. Seron, J.A. De Dona, "Sensor Fault-Tolerant Vector Control Of Induction Motors", *Published In IET Control Theory And Applications, Received On 8th September 2009, Revised On 7th April 2010, Doi: 10.1049/Iet-Cta.2009.0464*

63. Biranchi Narayan Kar, K.B. Mohanty, Madhu Singh, "Indirect Vector Control Of Induction Motor Using Fuzzy Logic Controller", *978-1-4244-8782-0/11/$26.00 ©2011 IEEE*
64. Chintan Patel, Rajeevan P. P., Anubrata Dey, Rijil Ramchand, K. Gopakumar, and Marian P. Kazmierkowski, "Fast Direct Torque Control of an Open-End Induction Motor Drive Using 12-Sided Polygonal Voltage Space Vectors*", IEEE Transactions On Power Electronics, Vol. 27, No. 1, January 2012*
65. Donald Grahame Holmes, Brendan Peter Mcgrath, and Stewart Geoffrey Parker, "Current Regulation Strategies For Vector-Controlled Induction Motor Drives", *IEEE Transactions On Industrial Electronics, Vol. 59, No. 10, October 2012*
66. A. V. Ravi Teja, Chandan Chakraborty, Suman Maiti, and Yoichi Hori, "A New Model Reference Adaptive Controller For Four Quadrant Vector Controlled Induction Motor Drives", *IEEE Transactions On Industrial Electronics, Vol. 59, No. 10, October 2012*
67. Bimal. K.Bose – "Modern Power Electronics & AC Drives", Prentice Hall
68. Ned Mohan, Tore M. Undeland, William P.Robbins – "Power Electronics, Converters, Apllication & Design", John Wiley & Sons
69. DS1104 R&D Controller Board, "Features", Release 7.3 – May 2012, www.dspace.com
70. DS1104 R&D Controller Board, "Hardware Installation and Configuration for DS1104 and CP1104/CLP1104 Connector Panels", Release 7.2 – November 2011
71. DS1104 R&D Controller Board, "RTI Reference", Release 7.3 – May 2012